Applications of Wavelets to Partial Differential Equations

Mani Mehra

Department of Mathematics and Statistics

McMaster University

Inspiring Innovation and Discovery

1. Part 1: Wavelet-Taylor Galerkin method for PDE's on flat geometries
   - Motivation
   - Wavelet-Taylor Galerkin method
   - Conclusion and future plan

2. Part 2: Adaptive wavelet collocation method for PDEs on manifolds
   - Motivation
   - Adaptive wavelet collocation method on the sphere
   - Conclusions and future directions

Collaborator

- Dr. B. V. Rathish Kumar (Indian Institute of Technology)

Why Wavelets?

- Efficient way to compress the smooth data except in localized region

Example

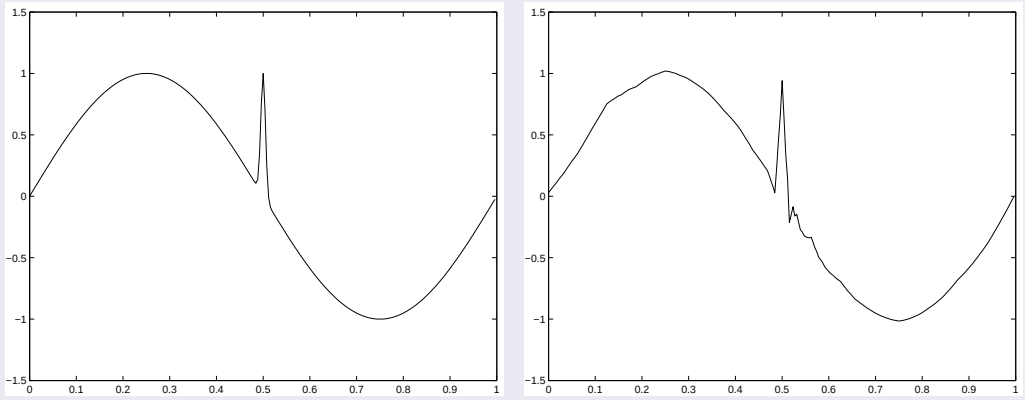

Initial function and approximate initial function with the wavelet threshold $\epsilon = 10^{-3}$, constructed with 13 retained wavelet coefficients out of original $2^8 = 256$

Why Wavelets?

- Efficient way to compress the smooth data except in localized region
- Good approximation properties
- Sparse representation of Calderon-Zygmond type operators
- Easy to control wavelet properties (e.g. smoothness, better accuracy near sharp gradients).

Why Wavelets?

- Efficient way to compress the smooth data except in localized region
- Good approximation properties
- Sparse representation of Calderon-Zygmond type operators
- Easy to control wavelet properties (e.g. smoothness, better accuracy near sharp gradients).

Why Wavelets?

- Efficient way to compress the smooth data except in localized region
- Good approximation properties
- Sparse representation of Calderon-Zygmond type operators
- Easy to control wavelet properties (e.g. smoothness, better accuracy near sharp gradients).

Why Taylor-Galerkin method?

- Higher order time accurate method
- Improved stability properties

Why Taylor-Galerkin method?

- Higher order time accurate method
- Improved stability properties

Why wavelet-Taylor Galerkin method?

- Successive powers of time iteration matrix become sparser with increasing time

Example

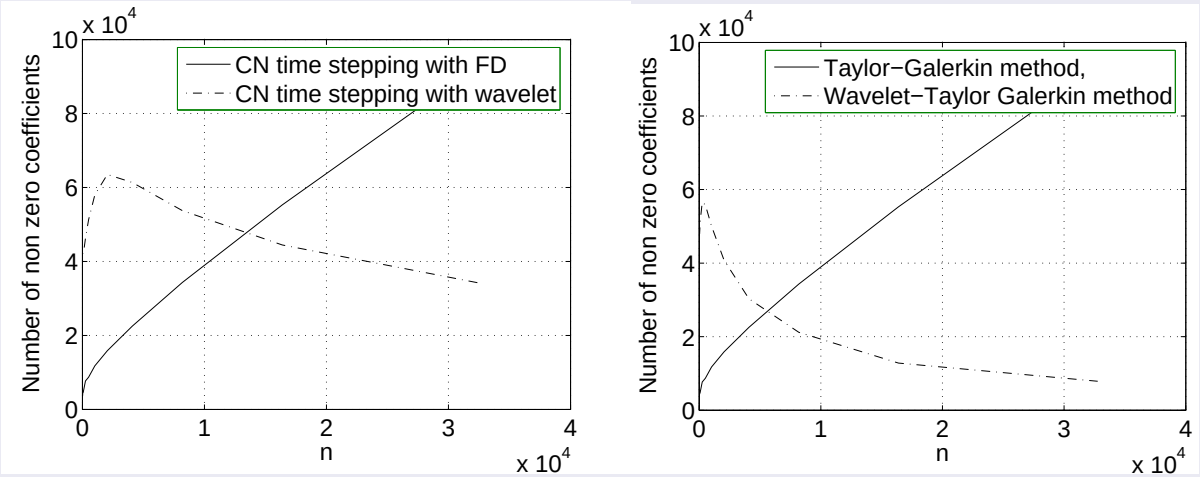

- Improved convergence and stability properties as compared to wavelet Galerkin method and Taylor-Galerkin method .

Example

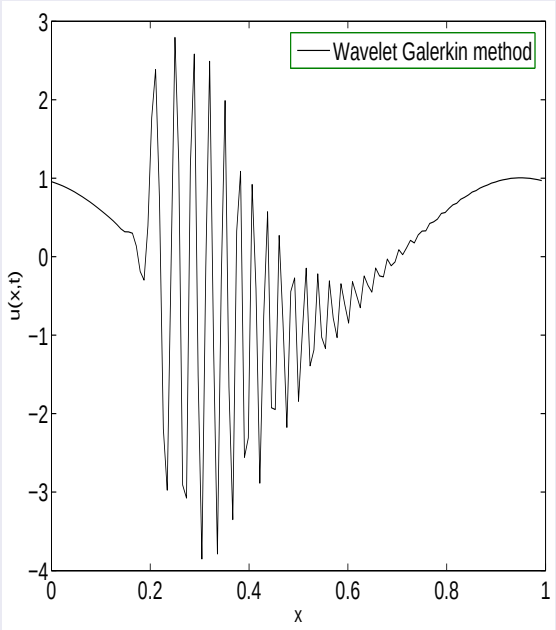

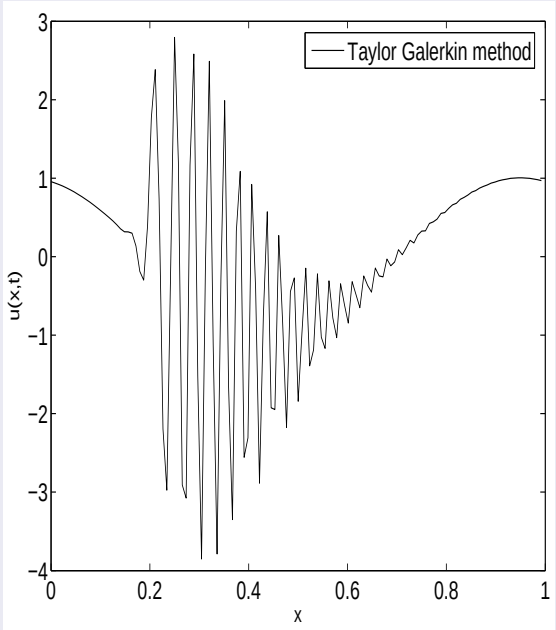

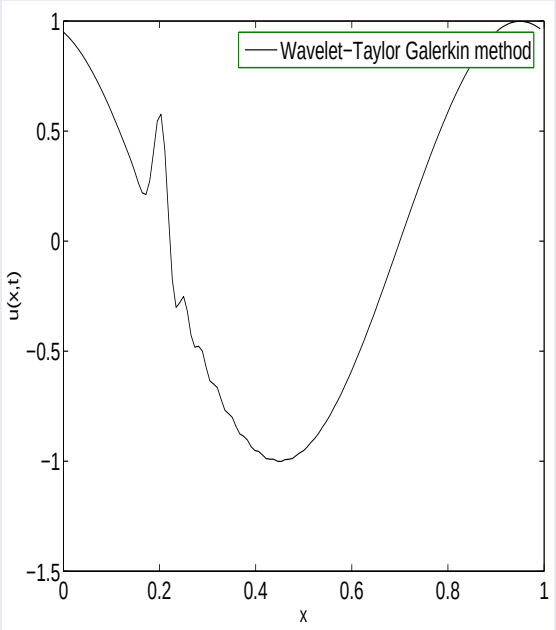

Ref:M. Mehra, B.V. Rathish Kumar, Time-accurate solution of advection diffusion problems by wavelet-Taylor Galerkin method, **Communications in Numerical Methods in Engineering**, Vol. 21 (2005)

- Improved convergence and stability properties as compared to wavelet Galerkin method and Taylor-Galerkin method .

Example

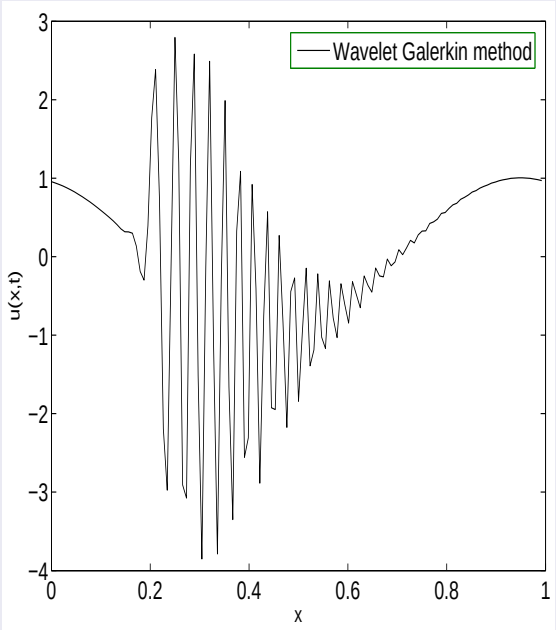

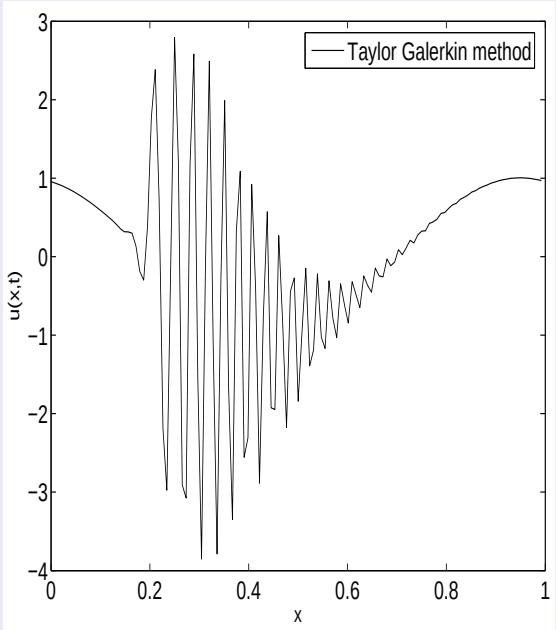

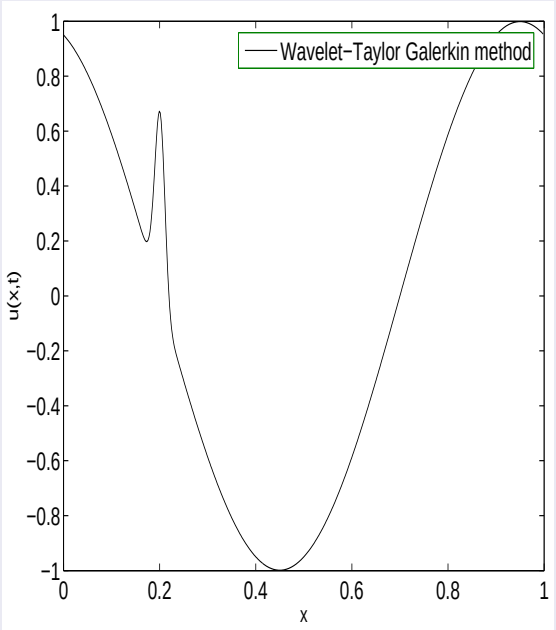

Ref:M. Mehra, B.V. Rathish Kumar, Time-accurate solution of advection diffusion problems by wavelet-Taylor Galerkin method, **Communications in Numerical Methods in Engineering**, Vol. 21 (2005)

Multiresolution Analysis of $L_2(\mathbb{R})$

Definition

MRA is characterized by the following axioms

- $\{0\} \subset \cdots \subset \mathcal{V}^{-1} \subset \mathcal{V}^0 \subset \mathcal{V}^1 \cdots \subset L_2(\mathbb{R})$
- $\overline{\bigcup_{j=-\infty}^{j=\infty} \mathcal{V}^j} = L_2(\mathbb{R})$
- $\bigcap_{j\in\mathbb{Z}} \mathcal{V}^j = \{0\}$
- Invariance to dilations, *i.e* $f \in \mathcal{V}^j$ iff $f(2(.)) \in \mathcal{V}^{j+1}$
- Invariance to translations, *i.e* $\{\phi_k^0$ (scaling function) $= \phi(x-k) | k \in \mathbb{Z}\}$ is an orthonormal basis for $\mathcal{V}^0$

Define $\mathcal{W}^j = \{\psi_k^j$ (wavelet) $| k \in \mathbb{Z}\}$ to be the complement of $\mathcal{V}^j$ in $\mathcal{V}^{j+1}$, where $\mathcal{V}^{j+1} = \mathcal{V}^j + \mathcal{W}^j$.

Each member of the wavelet family is determined by the set of constants a_k from the dilation equation

$$\phi_0^0 = \sum_{k=0}^{D-1} a_k \phi_k^1 \Longrightarrow \phi(x) = \sqrt{2} \sum_{k=0}^{D-1} a_k \phi(2x-k)$$

and by the set of constants b_k from the wavelet equation

$$\psi_0^0 = \sum_{k=0}^{D-1} b_k \phi_k^1 \Longrightarrow \psi(x) = \sqrt{2} \sum_{k=0}^{D-1} b_k \phi(2x-k)$$

$$b_k = (-1)^k a_{D-1-k}, k = 0, 1, \cdots, D-1.$$

$$\int_{-\infty}^{\infty} \phi(x)dx = 1 \quad \int_{-\infty}^{\infty} \phi_k^j(x)\phi_l^j(x)dx = \delta_{k,l}$$

$$\int_{-\infty}^{\infty} \psi_k^i(x)\psi_l^j(x)dx = \delta_{i,j}\delta_{k,l} \quad \int_{-\infty}^{\infty} \phi_k^i(x)\psi_l^j(x)dx = 0 \quad j \geq i$$

Orthogonal projections

$$P_{\mathcal{V}^j} f(x) = \sum_{k=-\infty}^{\infty} c_k^j \phi_k^j(x), \quad x \in \mathbb{R}$$

$$P_{\mathcal{W}^j} f(x) = \sum_{k=-\infty}^{\infty} d_k^j \psi_k^j(x), \quad x \in \mathbb{R}$$

Wavelet decomposition

$$P_{\mathcal{V}^j} f = P_{\mathcal{V}^{J_0}} f + \sum_{j=J_0}^{J-1} P_{\mathcal{W}^j} f$$

Important family of wavelets

Daubechies wavelet with different compact support, Coiflet, Semi-orthogonal wavelet, Battle-Lemarie's wavelets, biorthogonal wavelet, interpolats.

Daubechies scaling and wavelet functions

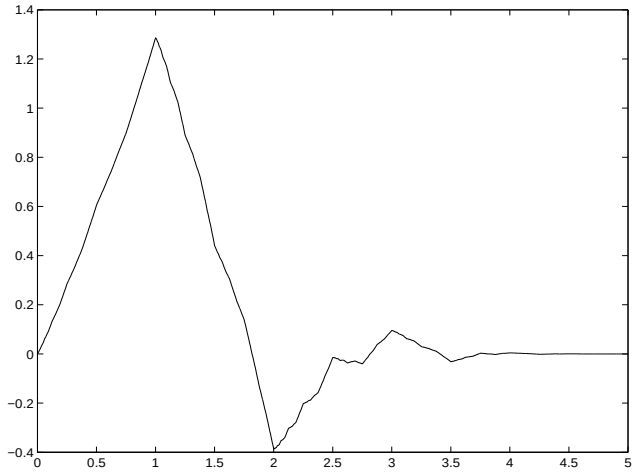

Scaling function ϕ for $M = 3$

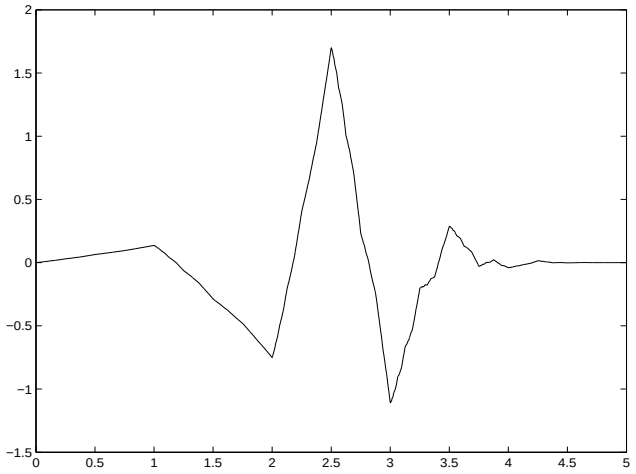

Wavelet function ψ for $M = 3$

Important family of wavelets

Daubechies wavelet with different compact support, Coiflet, Semi-orthogonal wavelet, Battle-Lemarie's wavelets, biorthogonal wavelet, interpolats.

Daubechies scaling and wavelet functions

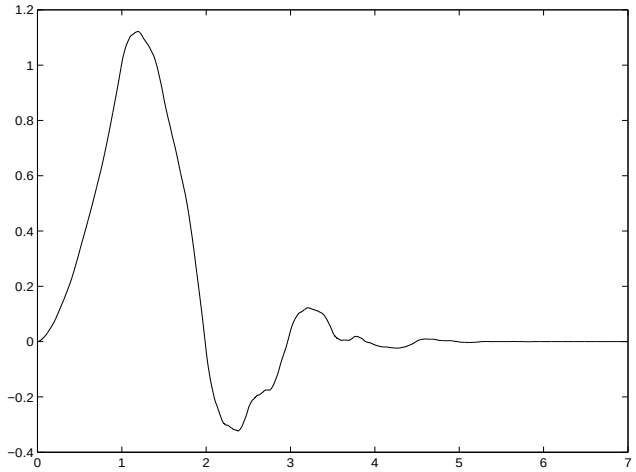

Scaling function ϕ for $M = 4$

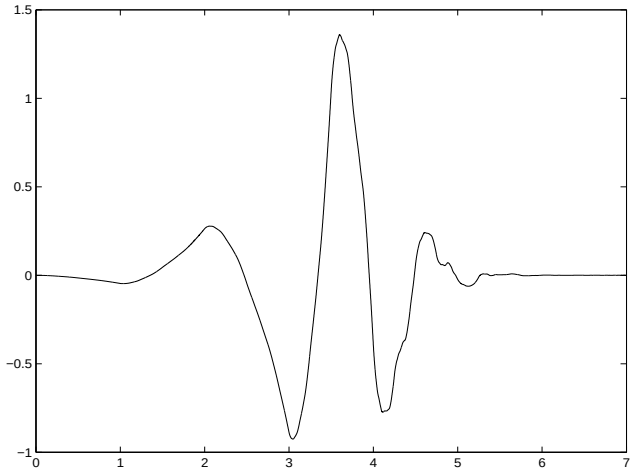

Wavelet function ψ for $M = 4$

Wavelet Expansion

Since space $\mathcal{V}^J$ is decomposed into wavelet space $\mathcal{V}^{J_0} + \mathcal{W}^{J_0} + \mathcal{W}^{J_0-1} + \cdots + \mathcal{W}^{J-1}$ Using this relation we obtain

$$P_{\mathcal{V}^J} f(x) = \sum_{k=-\infty}^{\infty} c_k^{J_0} \phi_k^{J_0}(x) + \sum_{j=J_0}^{J-1} \sum_{k=-\infty}^{\infty} d_k^j \psi_k^j(x).$$

Where J_0 satisfy $0 \leq J_0 \leq J$.Where the coefficients $c_k^{J_0}$ and d_k^j are given by

$$c_k^{J_0} = \int_{-\infty}^{\infty} f(x)\phi_k^{J_0}(x)dx$$

$$d_k^j = \int_{-\infty}^{\infty} f(x)\psi_k^j(x)dx, \; j = J_0, \cdots, j-1$$

An estimate for the decay of wavelet coefficients

The decay of wavelet coefficients is expressed in the following theorem.

Theorem

Let $M = D/2$ be the number of vanishing moments for a wavelet ψ_k^j and let $f \in C^M(\mathbb{R})$. Then the wavelet coefficients decay as follows:

$$|d_k^j| \leq C_M 2^{-j(M+\frac{1}{2})} max_{\xi \in I_{j,k}} |f^{(M)}(\xi)|.$$

Where C_M is a constant independent of j, k and f and $I_{j,k}$ denotes the support of ψ_k^j.

$$\|f - P_{\mathcal{V}^J} f\| = \|\sum_{j=J}^{\infty} \sum_{k=-\infty}^{\infty} d_k^j \psi_k^j(x)\| = O(2^{-JM})$$

Our Model

Consider the equations of the form

$$u_t = \mathcal{A}u + \mathcal{N}g(u) + f(x, y)$$

with suitable initial and boundary conditions. Here $\mathcal{A}$ and $\mathcal{N}$ are constant-coefficient differential operators that do not depend upon time t and the function $g(u)$ is non-linear.

Approximation in time

To obtain a second order method the Taylor series is taken as

$$\frac{u^n - u^{n-1}}{\delta t} = u_t^{n-1} + \frac{\delta t}{2} u_{tt}^{n-1} + O(\delta t^2)$$
$$\frac{u^{n-1} - u^n}{\delta t} = -u_t^n + \frac{\delta t}{2} u_{tt}^n + O(\delta t^2)$$

Combining the above expressions gives

$$\frac{u^n - u^{n-1}}{\delta t} = \frac{1}{2}(u_t^{n-1} + u_t^n) + \frac{\delta t}{4}(u_{tt}^{n-1} - u_{tt}^n) + O(\delta t^2)$$

Then using our model problem,

$$u_t = -\mathcal{A}u, \quad u_{tt} = \mathcal{A}^2 u$$

the initial boundary value problem is converted in to a sequence of boundary value problems

$$u^n = \mathcal{T} u^{n-1}$$
$$u(x, 0) = u^0$$
$$\delta t = t^*/N, t_n = n\delta t, n = 1, \cdots, N+1$$

Approximation in space

The variational formulation of the wavelet Taylor-Galerkin scheme is

$$\text{Given } u_h^0 \in \mathbb{V}^j$$

$$\mathcal{B}(u_h^n, v_h) - \frac{\delta t}{2}\mathcal{D}(u_h^n, v_h) + \frac{\delta t^2}{4}\mathcal{C}(u_h^n, v_h) = \mathcal{B}(u_h^{n-1}, v_h) + \frac{\delta t}{2}\mathcal{D}(u_h^{n-1}, v_h) + \frac{\delta t^2}{4}\mathcal{C}(u_h^n, v_h)$$

Where the bilinear forms $\mathcal{B}$, $\mathcal{C}$ and $\mathcal{D}$ are defined by

$$\mathcal{B}, \mathcal{C}, \mathcal{D} : V \times V \to \mathbb{C}$$

$$\mathcal{B}(u, v) = (u, v), \quad \mathcal{C}(u, v) = (\mathcal{A}u, \mathcal{A}v), \quad \mathcal{D}(u, v) = (\mathcal{A}u, v)$$

Advection Equation M. Holmstrom and J. Walden have applied adaptive wavelet methods on such type of PDEs. But by our approach of FW-TGM method we are taking the advantage of time accurate scheme as well as wavelet capabilities of compression to produce fast algorithm based on fast matrix vector product in terms of sparsity.

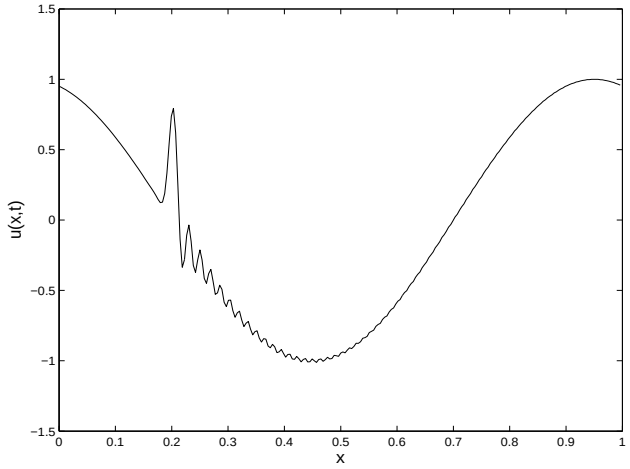

Solution at $t = .3$ using $j = 8$ by F-WGM

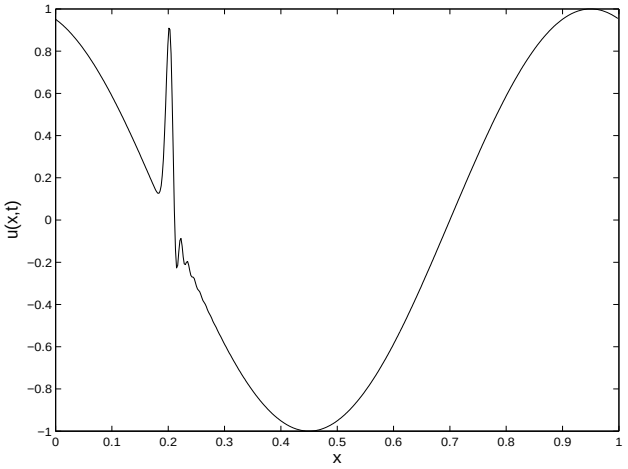

Solution at $t = .3$ using $j = 9$ by F-WGM

Advection Equation M. Holmstrom and J. Walden have applied adaptive wavelet methods on such type of PDEs. But by our approach of FW-TGM method we are taking the advantage of time accurate scheme as well as wavelet capabilities of compression to produce fast algorithm based on fast matrix vector product in terms of sparsity.

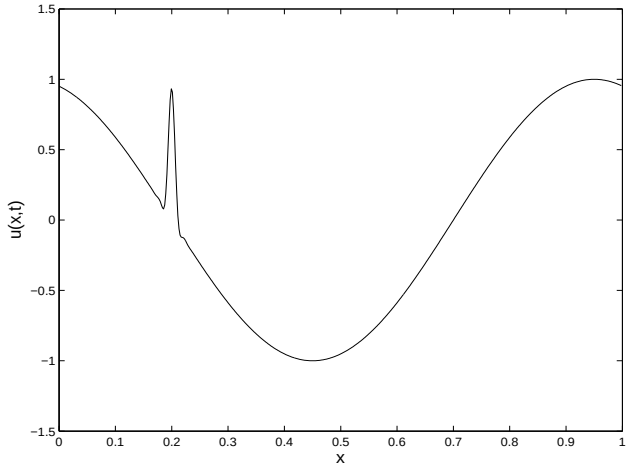

Solution at $t = .3$, $\epsilon_M = 0$, $\epsilon_v = 0$ by FW-TGM

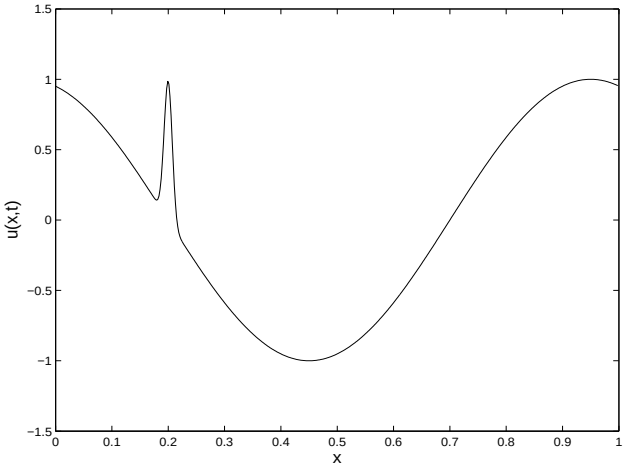

Solution at $t = .3$, $\epsilon_M = 0$, $\epsilon_v = 10^{-6}$ by FW-TGM

Moreover, near the spike error in FW-TGM method is small. From this we can conclude that near the sharp gradients we can take the advantage of time accuracy and compression properties of wavelet in FW-TGM method.

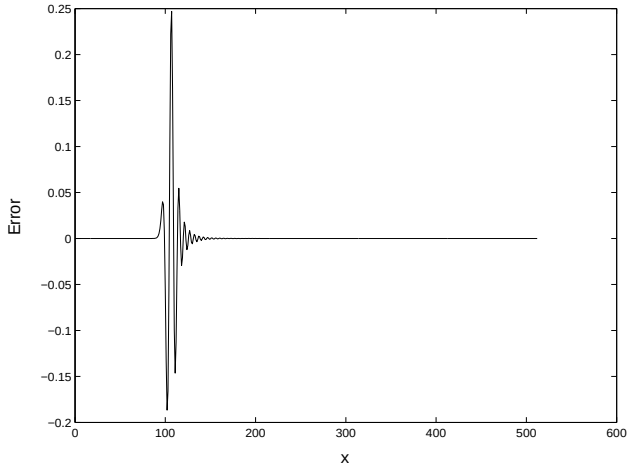

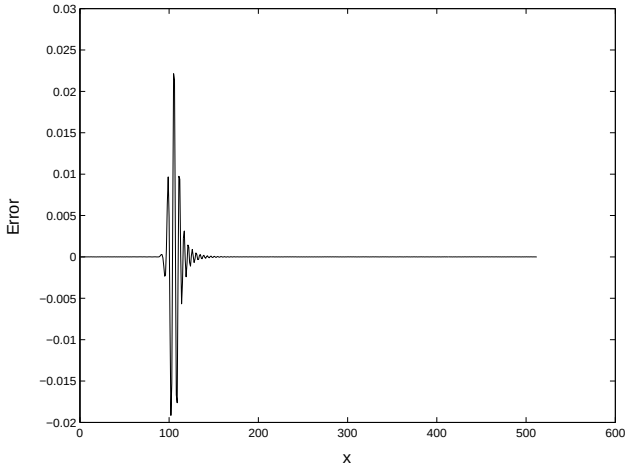

$D = 6$ using F-WGM $D = 6$ using FW-TGM

Ref: B. V. Rathish Kumar, Mani Mehra, Time accurate Fast Wavelet-Taylor Galerkin method for partial differential equations, **Numerical methods for partial differential equations**, Vol. 22 (2) (2005) pp. 274-295.

Moreover, near the spike error in FW-TGM method is small. From this we can conclude that near the sharp gradients we can take the advantage of time accuracy and compression properties of wavelet in FW-TGM method.

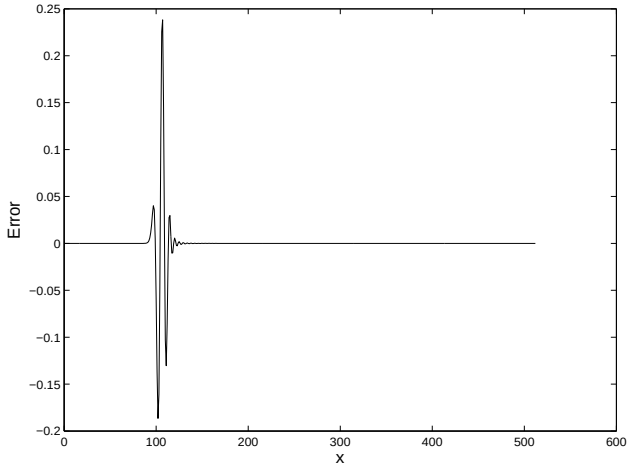

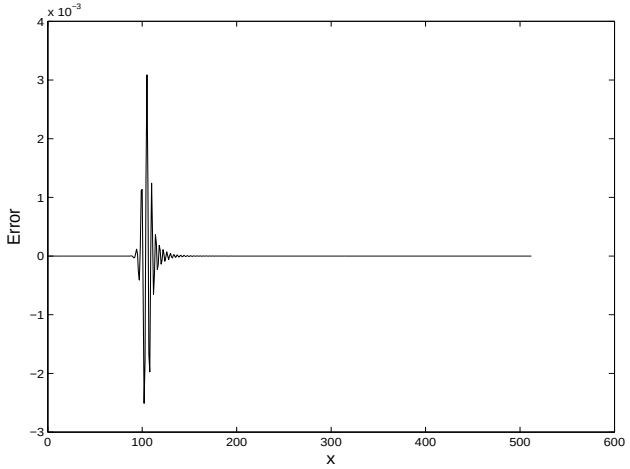

$D = 10$ using F-WGM $D = 10$ using FW-TGM

Ref: B. V. Rathish Kumar, Mani Mehra, Time accurate Fast Wavelet-Taylor Galerkin method for partial differential equations, **Numerical methods for partial differential equations**, Vol. 22 (2) (2005) pp. 274-295.

Inviscid Burgers equation (quasilinear hyperbolic conservation equation)

Case 1: Initial condition $u(x,0) = \sin(2\pi x)$. The solution due to FD scheme develops local oscillations while the solution due to FW-TGM continues to be smooth.

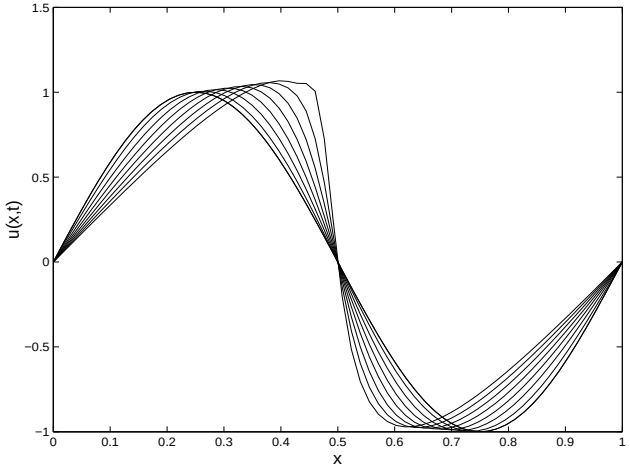

Solutions at various time using FD

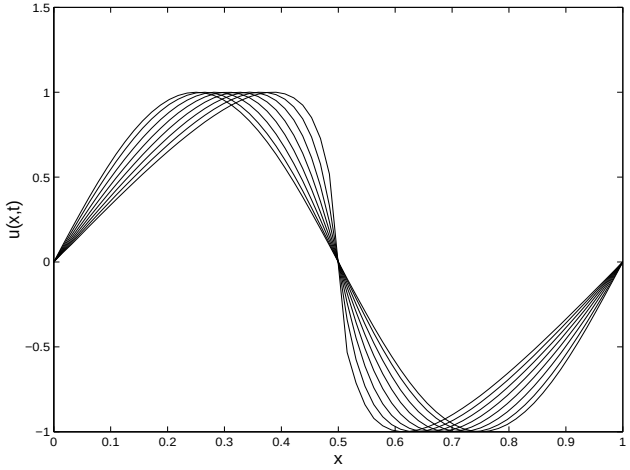

Solutions at various time using FW-TGM

Inviscid Burgers equation (quasilinear hyperbolic conservation equation)

Case 2: Here we are using initial condition

$$u(x,0) = \begin{cases} 1+x & -1 \le x \le 0 \\ 1-x & 0 \le x \le 1 \end{cases}$$

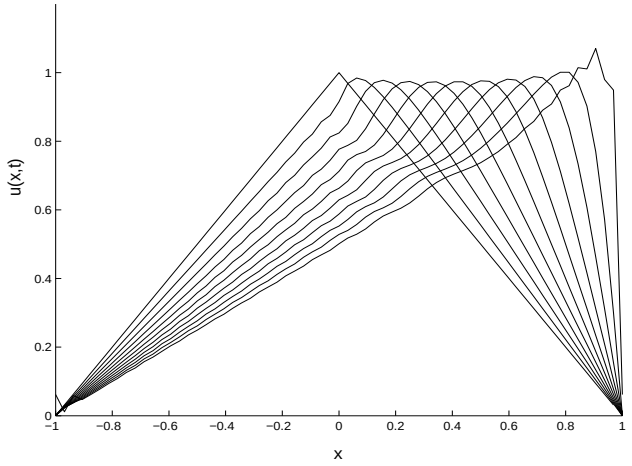

Local oscillation near shock using FW-TGM

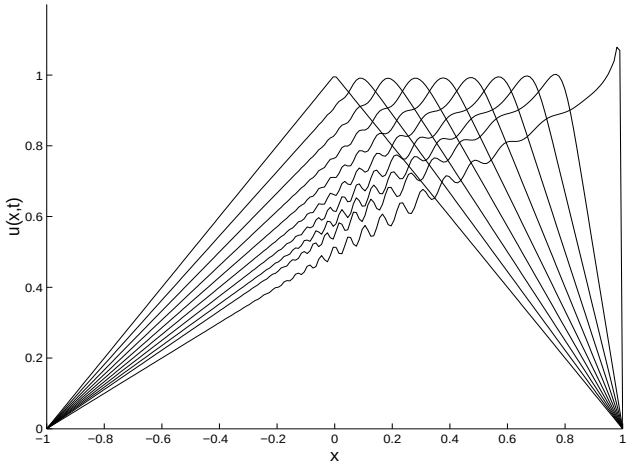

Global oscillation using Fourier-Galerkin

The Navier-Stokes equations

A two-dimensional incompressible viscous flow is described by the Navier-Stokes equations. In vorticity/stream-function formulation:

$$-\Delta\psi = \omega$$

$$\frac{\partial\omega}{\partial t} + J(\psi,\omega) = \nu\nabla\omega + \text{curl}f$$

where ω is the vorticity field (curl of the non-divergent velocity field), ψ the stream function, f a forcing term and $J(\psi,\omega) = \psi_y\omega_x - \psi_x\omega_y$ the two-dimensional Jacobian operator. Rewriting these equations as follows:

$$-\Delta\psi = \omega$$

$$\frac{\partial\omega}{\partial t} = \nu\nabla\omega + s, \quad s = \text{curl}f - J(\psi,\omega)$$

Wavelet-Taylor Galerkin method for Navier-Stokes Split the problem into three subproblems: solve a Poisson equation to obtain stream function from the vorticity, evaluate the non-linear term, integrate the heat equation.
Starting from $\tilde{\omega}^n$ at time $t = n\delta t$

- Compute $\tilde{\psi}^n$ by solving Poisson equation. Here the numerical solution has been searched as the long time asymptotic solution of the heat equation.
- Perform inverse wavelet transform to obtain nodal values ψ^n and ω^n.
- Compute the nonlinear r.h.s s^n by collocation approach using a second-order, energy enstrophy conserving, Arakawas' scheme.
- Compute the $\tilde{s}^n$ by s^n.
- Finally solve the heat equation using the wavelet-Taylor Galerkin schemes to obtain $\tilde{\omega}^{n+1}$.

Wavelet-Taylor Galerkin method for Navier-Stokes Split the problem into three subproblems: solve a Poisson equation to obtain stream function from the vorticity, evaluate the non-linear term, integrate the heat equation.
Starting from $\tilde{\omega}^n$ at time $t = n\delta t$

- Compute $\tilde{\psi}^n$ by solving Poisson equation. Here the numerical solution has been searched as the long time asymptotic solution of the heat equation.
- Perform inverse wavelet transform to obtain nodal values ψ^n and ω^n.
- Compute the nonlinear r.h.s s^n by collocation approach using a second-order, energy enstrophy conserving, Arakawas' scheme.
- Compute the $\tilde{s}^n$ by s^n.
- Finally solve the heat equation using the wavelet-Taylor Galerkin schemes to obtain $\tilde{\omega}^{n+1}$.

Wavelet-Taylor Galerkin method for Navier-Stokes Split the problem into three subproblems: solve a Poisson equation to obtain stream function from the vorticity, evaluate the non-linear term, integrate the heat equation.
Starting from $\tilde{\omega}^n$ at time $t = n\delta t$

- Compute $\tilde{\psi}^n$ by solving Poisson equation. Here the numerical solution has been searched as the long time asymptotic solution of the heat equation.
- Perform inverse wavelet transform to obtain nodal values ψ^n and ω^n.
- Compute the nonlinear r.h.s s^n by collocation approach using a second-order, energy enstrophy conserving, Arakawas' scheme.
- Compute the $\tilde{s}^n$ by s^n.
- Finally solve the heat equation using the wavelet-Taylor Galerkin schemes to obtain $\tilde{\omega}^{n+1}$.

Wavelet-Taylor Galerkin method for Navier-Stokes Split the problem into three subproblems: solve a Poisson equation to obtain stream function from the vorticity, evaluate the non-linear term, integrate the heat equation.
Starting from $\tilde{\omega}^n$ at time $t = n\delta t$

- Compute $\tilde{\psi}^n$ by solving Poisson equation. Here the numerical solution has been searched as the long time asymptotic solution of the heat equation.
- Perform inverse wavelet transform to obtain nodal values ψ^n and ω^n.
- Compute the nonlinear r.h.s s^n by collocation approach using a second-order, energy enstrophy conserving, Arakawas' scheme.
- Compute the $\tilde{s}^n$ by s^n.
- Finally solve the heat equation using the wavelet-Taylor Galerkin schemes to obtain $\tilde{\omega}^{n+1}$.

Wavelet-Taylor Galerkin method for Navier-Stokes Split the problem into three subproblems: solve a Poisson equation to obtain stream function from the vorticity, evaluate the non-linear term, integrate the heat equation.
Starting from $\tilde{\omega}^n$ at time $t = n\delta t$

- Compute $\tilde{\psi}^n$ by solving Poisson equation. Here the numerical solution has been searched as the long time asymptotic solution of the heat equation.
- Perform inverse wavelet transform to obtain nodal values ψ^n and ω^n.
- Compute the nonlinear r.h.s s^n by collocation approach using a second-order, energy enstrophy conserving, Arakawas' scheme.
- Compute the $\tilde{s}^n$ by s^n.
- Finally solve the heat equation using the wavelet-Taylor Galerkin schemes to obtain $\tilde{\omega}^{n+1}$.

Numerical simulation

The numerical experiment we present studies the merging of two same sign vortices. It concerns free decaying turbulence (no forcing term). The initial condition for the simulation considered is

$$\omega(x,y) = \sum_{i=1}^{i=3} A_i exp(-((x-x_i)^2 + (y-y_i)^2)/\sigma_i^2)$$

with variables $\sigma_i = 1/\pi$, amplitudes $A_1 = A_2 = -2A_3 = \pi$, and positions $x_1 = 3\pi/4, x_2 = x_3 = 5\pi/4$,
$y_1 = y_2 = \pi, y_3 = \pi(1 + 1/(9\sigma_2))$. In fully developed two-dimensional turbulent flows the chance of vortex merging increases with the density of vortices. Here with only three vortices we need this specific configuration to ensure a rapid merger.

In a $2\pi \times 2\pi$ box, three vortices with a Gaussian vorticity profile are present two are positive with the same intensity (π), one is negative with half the intensity of others.

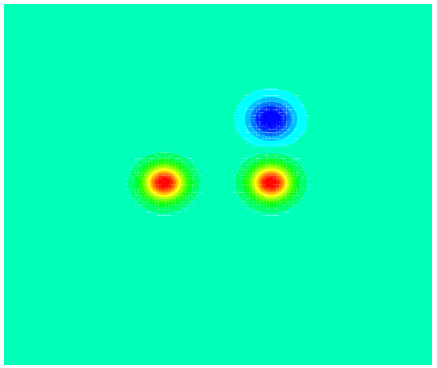

Three vortex interaction: initial state (t=0)

Further parameters are $J = 8, \delta t = 2.5 \times 10^{-3}$, $\nu = 5 \times 10^{-5}$. The turnover time of one of the positive vortices is initially $T = 4.0$, and the initial Reynolds number based on the circulation of one of the positive vortices is $Re = 2 \times 10^4$. The thresholds used in the wavelet compression are $\epsilon_v = 10^{-8}, \epsilon_M = 10^{-8}$.

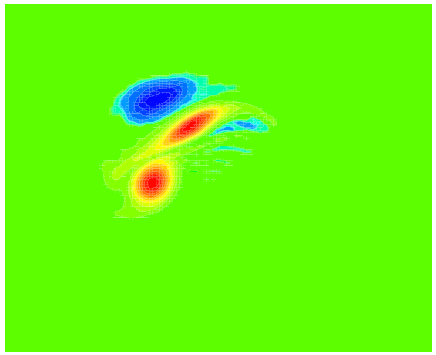
t=10

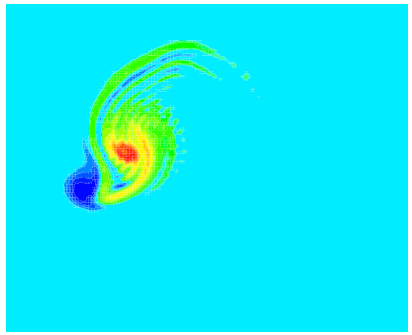
t=20

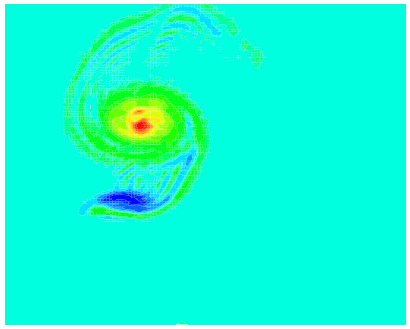
t=30

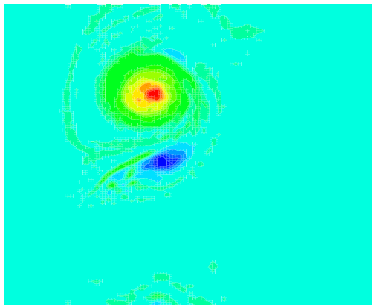
t=40

Three vortex interaction at different times

Ref: B. V. Rathish Kumar, Mani Mehra, A Time-Accurate pseudo-wavelet scheme for Parabolic and Hyperbolic PDE's, **Nonlinear Analysis**, Vol. 63 (2005) pp. e345-e356.

Conclusions

Wavelet-Taylor Galerkin method:

- Space and time accurate method
- Taking advantage of wavelet compression of operator as well as localized function (e.g Gaussian) therefore computationally efficient
- Method shows Improved stability properties

Future plans

- Incorporation of space-time adaptive features to the newly proposed wavelet-Taylor Galerkin method

Conclusions

Wavelet-Taylor Galerkin method:

- Space and time accurate method
- Taking advantage of wavelet compression of operator as well as localized function (e.g Gaussian) therefore computationally efficient
- Method shows Improved stability properties

Future plans

- Incorporation of space-time adaptive features to the newly proposed wavelet-Taylor Galerkin method

Conclusions

Wavelet-Taylor Galerkin method:

- Space and time accurate method
- Taking advantage of wavelet compression of operator as well as localized function (e.g Gaussian) therefore computationally efficient
- Method shows Improved stability properties

Future plans

- Incorporation of space-time adaptive features to the newly proposed wavelet-Taylor Galerkin method

Conclusions

Wavelet-Taylor Galerkin method:

- Space and time accurate method
- Taking advantage of wavelet compression of operator as well as localized function (e.g Gaussian) therefore computationally efficient
- Method shows Improved stability properties

Future plans

- Incorporation of space-time adaptive features to the newly proposed wavelet-Taylor Galerkin method

Conclusions

Wavelet-Taylor Galerkin method:

- Space and time accurate method
- Taking advantage of wavelet compression of operator as well as localized function (e.g Gaussian) therefore computationally efficient
- Method shows Improved stability properties

Future plans

- Incorporation of space-time adaptive features to the newly proposed wavelet-Taylor Galerkin method

Conclusions

Wavelet-Taylor Galerkin method:

- Space and time accurate method
- Taking advantage of wavelet compression of operator as well as localized function (e.g Gaussian) therefore computationally efficient
- Method shows Improved stability properties

Future plans

- Incorporation of space-time adaptive features to the newly proposed wavelet-Taylor Galerkin method

Collaborator

- Nicholas Kevlahan (McMaster University)

Why general manifolds?(e.g. Sphere)

- Application of adaptive wavelet collocation method (AWCM) to the problems of geodesy, climatology, meteorology (Representative examples include forecasting the moisture and cloud water fields in numerical weather prediction).
- Many PDEs arise from mean curvature flow, surface diffusion flow and Willmore flow on the sphere.

Why general manifolds?(e.g. Sphere)

- Application of adaptive wavelet collocation method (AWCM) to the problems of geodesy, climatology, meteorology (Representative examples include forecasting the moisture and cloud water fields in numerical weather prediction).
- Many PDEs arise from mean curvature flow, surface diffusion flow and Willmore flow on the sphere.

Why general manifolds?(e.g. Sphere)

- Application of adaptive wavelet collocation method (AWCM) to the problems of geodesy, climatology, meteorology (Representative examples include forecasting the moisture and cloud water fields in numerical weather prediction).
- Many PDEs arise from mean curvature flow, surface diffusion flow and Willmore flow on the sphere.

Why general manifolds?(e.g. Sphere)

- Application of adaptive wavelet collocation method (AWCM) to the problems of geodesy, climatology, meteorology (Representative examples include forecasting the moisture and cloud water fields in numerical weather prediction).
- Many PDEs arise from mean curvature flow, surface diffusion flow and Willmore flow on the sphere.

Why wavelets?

- Fast $O(\mathcal{N})$ transform.
- Dynamic grid adaption to the local irregularities of the solution.
  (This situation arises e.g. in the tracking of storms or fronts for the simulation of global atmospheric dynamics).

Why wavelets?

- Fast $O(\mathcal{N})$ transform.
- Dynamic grid adaption to the local irregularities of the solution.
  (This situation arises e.g. in the tracking of storms or fronts for the simulation of global atmospheric dynamics).

Why wavelets?

- Fast $O(\mathcal{N})$ transform.
- Dynamic grid adaption to the local irregularities of the solution.
  (This situation arises e.g. in the tracking of storms or fronts for the simulation of global atmospheric dynamics).

Why wavelets on manifolds? (e.g. spherical wavelets)

- Spherical triangular grids (quasi uniform triangulations) avoid the pole problem.
  Conventional grid–uniform longitude-latitude grid
  - Problem- Singularity of coordinate system near the poles
  - Solution-
    - Necessary to introduce auxiliary coordinate system.
    - Another solution is to avoid the introduction of the 'metric term' which are unbounded near the poles.
- To solve PDEs efficiently using adaptivity on general manifold by wavelet methods was an open problem.
- Past applications of wavelets to turbulence have been mainly restricted to flat geometries which severely limits for geophysical applications.

Why wavelets on manifolds? (e.g. spherical wavelets)

- Spherical triangular grids (quasi uniform triangulations) avoid the pole problem.
  Conventional grid–uniform longitude-latitude grid
  - Problem- Singularity of coordinate system near the poles
  - Solution-
    - Necessary to introduce auxiliary coordinate system.
    - Another solution is to avoid the introduction of the 'metric term' which are unbounded near the poles.
- To solve PDEs efficiently using adaptivity on general manifold by wavelet methods was an open problem.
- Past applications of wavelets to turbulence have been mainly restricted to flat geometries which severely limits for geophysical applications.

Why wavelets on manifolds? (e.g. spherical wavelets)

- Spherical triangular grids (quasi uniform triangulations) avoid the pole problem.
  Conventional grid–uniform longitude-latitude grid
  - Problem- Singularity of coordinate system near the poles
  - Solution-
    - Necessary to introduce auxiliary coordinate system.
    - Another solution is to avoid the introduction of the 'metric term' which are unbounded near the poles.
- To solve PDEs efficiently using adaptivity on general manifold by wavelet methods was an open problem.
- Past applications of wavelets to turbulence have been mainly restricted to flat geometries which severely limits for geophysical applications.

Why wavelets on manifolds? (e.g. spherical wavelets)

- Spherical triangular grids (quasi uniform triangulations) avoid the pole problem.
  Conventional grid–uniform longitude-latitude grid
  - Problem- Singularity of coordinate system near the poles
  - Solution-
    - Necessary to introduce auxiliary coordinate system.
    - Another solution is to avoid the introduction of the 'metric term' which are unbounded near the poles.
- To solve PDEs efficiently using adaptivity on general manifold by wavelet methods was an open problem.
- Past applications of wavelets to turbulence have been mainly restricted to flat geometries which severely limits for geophysical applications.

Why wavelets on manifolds? (e.g. spherical wavelets)

- Spherical triangular grids (quasi uniform triangulations) avoid the pole problem.
  Conventional grid–uniform longitude-latitude grid
  - Problem- Singularity of coordinate system near the poles
  - Solution-
    - Necessary to introduce auxiliary coordinate system.
    - Another solution is to avoid the introduction of the 'metric term' which are unbounded near the poles.
- To solve PDEs efficiently using adaptivity on general manifold by wavelet methods was an open problem.
- Past applications of wavelets to turbulence have been mainly restricted to flat geometries which severely limits for geophysical applications.

Why wavelets on manifolds? (e.g. spherical wavelets)

- Spherical triangular grids (quasi uniform triangulations) avoid the pole problem.
  Conventional grid–uniform longitude-latitude grid
  - Problem- Singularity of coordinate system near the poles
  - Solution-
    - Necessary to introduce auxiliary coordinate system.
    - Another solution is to avoid the introduction of the 'metric term' which are unbounded near the poles.
- To solve PDEs efficiently using adaptivity on general manifold by wavelet methods was an open problem.
- Past applications of wavelets to turbulence have been mainly restricted to flat geometries which severely limits for geophysical applications.

Why wavelets on manifolds? (e.g. spherical wavelets)

- Spherical triangular grids (quasi uniform triangulations) avoid the pole problem.
  Conventional grid–uniform longitude-latitude grid
  - Problem- Singularity of coordinate system near the poles
  - Solution-
    - Necessary to introduce auxiliary coordinate system.
    - Another solution is to avoid the introduction of the 'metric term' which are unbounded near the poles.
- To solve PDEs efficiently using adaptivity on general manifold by wavelet methods was an open problem.
- Past applications of wavelets to turbulence have been mainly restricted to flat geometries which severely limits for geophysical applications.

Why wavelets on manifolds? (e.g. spherical wavelets)

- Spherical triangular grids (quasi uniform triangulations) avoid the pole problem.
  Conventional grid–uniform longitude-latitude grid
  - Problem- Singularity of coordinate system near the poles
  - Solution-
    - Necessary to introduce auxiliary coordinate system.
    - Another solution is to avoid the introduction of the 'metric term' which are unbounded near the poles.
- To solve PDEs efficiently using adaptivity on general manifold by wavelet methods was an open problem.
- Past applications of wavelets to turbulence have been mainly restricted to flat geometries which severely limits for geophysical applications.

Wavelet multiresolution analysis of $L_2(S)$

Definition

MRA is characterized by the following axioms

- $V^j \subset \mathcal{V}^{j+1}$ (subspaces are nested).
- $\overline{\bigcup_{j=-\infty}^{j=\infty} \mathcal{V}^j} = L_2(S)$.
- Each $\mathcal{V}^j$ has a Riesz basis of scaling function $\{\phi_k^j | k \in \mathcal{K}^j\}$.

Define $\mathcal{W}^j = \{\psi_m^j(\textit{wavelets}) | m \in \mathcal{M}^j\}$ to be the complement of $\mathcal{V}^j$ in $\mathcal{V}^{j+1}$, where $\mathcal{V}^{j+1} = \mathcal{V}^j \oplus \mathcal{W}^j$.

$$\phi_k^j = \sum_{l \in \mathcal{K}^{j+1}} h_{k,l}^j \phi_l^{j+1} \text{ (dilation equation)}$$

$$\psi_m^j = \sum_{l \in \mathcal{K}^{j+1}} g_{m,l}^j \phi_l^{j+1}, m \in \mathcal{M}^j \text{ (wavelet equation)}$$

Wavelet multiresolution analysis of $L_2(S)$

Definition

MRA is characterized by the following axioms

- $V^j \subset \mathcal{V}^{j+1}$ (subspaces are nested).
- $\overline{\bigcup_{j=-\infty}^{j=\infty} \mathcal{V}^j} = L_2(S)$.
- Each $\mathcal{V}^j$ has a Riesz basis of scaling function $\{\phi_k^j | k \in \mathcal{K}^j\}$.

Define $\mathcal{W}^j = \{\psi_m^j (\textit{wavelets}) | m \in \mathcal{M}^j\}$ to be the complement of $\mathcal{V}^j$ in $\mathcal{V}^{j+1}$, where $\mathcal{V}^{j+1} = \mathcal{V}^j \oplus \mathcal{W}^j$.

$$\phi_k^j = \sum_{l \in \mathcal{K}^{j+1}} h_{k,l}^j \phi_l^{j+1} \text{ (dilation equation)}$$

$$\psi_m^j = \sum_{l \in \mathcal{K}^{j+1}} g_{m,l}^j \phi_l^{j+1}, m \in \mathcal{M}^j \text{ (wavelet equation)}$$

Wavelet multiresolution analysis of $L_2(S)$

Definition

MRA is characterized by the following axioms

- $V^j \subset \mathcal{V}^{j+1}$ (subspaces are nested).
- $\overline{\bigcup_{j=-\infty}^{j=\infty} \mathcal{V}^j} = L_2(S)$.
- Each $\mathcal{V}^j$ has a Riesz basis of scaling function $\{\phi_k^j | k \in \mathcal{K}^j\}$.

Define $\mathcal{W}^j = \{\psi_m^j (\textit{wavelets}) | m \in \mathcal{M}^j\}$ to be the complement of $\mathcal{V}^j$ in $\mathcal{V}^{j+1}$, where $\mathcal{V}^{j+1} = \mathcal{V}^j \oplus \mathcal{W}^j$.

$$\phi_k^j = \sum_{l \in \mathcal{K}^{j+1}} h_{k,l}^j \phi_l^{j+1} \text{ (dilation equation)}$$

$$\psi_m^j = \sum_{l \in \mathcal{K}^{j+1}} g_{m,l}^j \phi_l^{j+1}, m \in \mathcal{M}^j \text{ (wavelet equation)}$$

Wavelet multiresolution analysis of $L_2(S)$

Definition

MRA is characterized by the following axioms

- $V^j \subset \mathcal{V}^{j+1}$ (subspaces are nested).
- $\overline{\bigcup_{j=-\infty}^{j=\infty} \mathcal{V}^j} = L_2(S)$.
- Each $\mathcal{V}^j$ has a Riesz basis of scaling function $\{\phi_k^j | k \in \mathcal{K}^j\}$.

Define $\mathcal{W}^j = \{\psi_m^j (\textit{wavelets}) | m \in \mathcal{M}^j\}$ to be the complement of $\mathcal{V}^j$ in $\mathcal{V}^{j+1}$, where $\mathcal{V}^{j+1} = \mathcal{V}^j \oplus \mathcal{W}^j$.

$$\phi_k^j = \sum_{l \in \mathcal{K}^{j+1}} h_{k,l}^j \phi_l^{j+1} \text{ (dilation equation)}$$

$$\psi_m^j = \sum_{l \in \mathcal{K}^{j+1}} g_{m,l}^j \phi_l^{j+1}, m \in \mathcal{M}^j \text{ (wavelet equation)}$$

Wavelet multiresolution analysis of $L_2(S)$

Definition

MRA is characterized by the following axioms

- $V^j \subset \mathcal{V}^{j+1}$ (subspaces are nested).
- $\overline{\bigcup_{j=-\infty}^{j=\infty} \mathcal{V}^j} = L_2(S)$.
- Each $\mathcal{V}^j$ has a Riesz basis of scaling function $\{\phi_k^j | k \in \mathcal{K}^j\}$.

Define $\mathcal{W}^j = \{\psi_m^j (\textit{wavelets}) | m \in \mathcal{M}^j\}$ to be the complement of $\mathcal{V}^j$ in $\mathcal{V}^{j+1}$, where $\mathcal{V}^{j+1} = \mathcal{V}^j \oplus \mathcal{W}^j$.

$$\phi_k^j = \sum_{l \in \mathcal{K}^{j+1}} h_{k,l}^j \phi_l^{j+1} \text{ (dilation equation)}$$

$$\psi_m^j = \sum_{l \in \mathcal{K}^{j+1}} g_{m,l}^j \phi_l^{j+1}, m \in \mathcal{M}^j \text{ (wavelet equation)}$$

Wavelet multiresolution analysis of $L_2(S)$

Definition

MRA is characterized by the following axioms

- $V^j \subset \mathcal{V}^{j+1}$ (subspaces are nested).
- $\overline{\bigcup_{j=-\infty}^{j=\infty} \mathcal{V}^j} = L_2(S)$.
- Each $\mathcal{V}^j$ has a Riesz basis of scaling function $\{\phi_k^j | k \in \mathcal{K}^j\}$.

Define $\mathcal{W}^j = \{\psi_m^j(\textit{wavelets}) | m \in \mathcal{M}^j\}$ to be the complement of $\mathcal{V}^j$ in $\mathcal{V}^{j+1}$, where $\mathcal{V}^{j+1} = \mathcal{V}^j \oplus \mathcal{W}^j$.

$$\phi_k^j = \sum_{l \in \mathcal{K}^{j+1}} h_{k,l}^j \phi_l^{j+1} \text{ (dilation equation)}$$

$$\psi_m^j = \sum_{l \in \mathcal{K}^{j+1}} g_{m,l}^j \phi_l^{j+1}, m \in \mathcal{M}^j \text{ (wavelet equation)}$$

Construction of spherical wavelets based on spherical triangular grids

The set of all vertices

$\mathcal{S}^j = \{p_k^j \in S : p_k^j = p_{2k}^{j+1} | k \in \mathcal{K}^j\}$ and $\mathcal{M}^j = \mathcal{K}^{j+1}/\mathcal{K}^j$.

Level 0

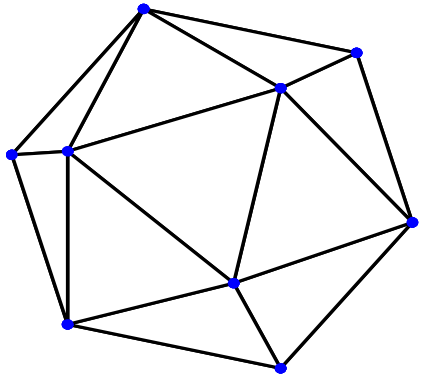

Dyadic icosahedral triangulation of the sphere

Construction of spherical wavelets based on spherical triangular grids

The set of all vertices

$\mathcal{S}^j = \{p_k^j \in S : p_k^j = p_{2k}^{j+1} | k \in \mathcal{K}^j\}$ and $\mathcal{M}^j = \mathcal{K}^{j+1}/\mathcal{K}^j$.

Level 1

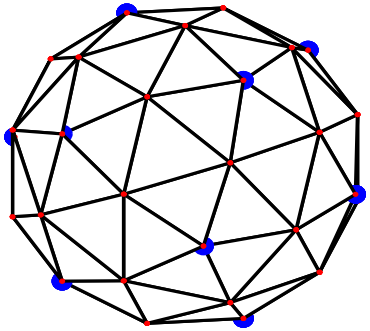

Dyadic icosahedral triangulation of the sphere

Fast wavelet transform

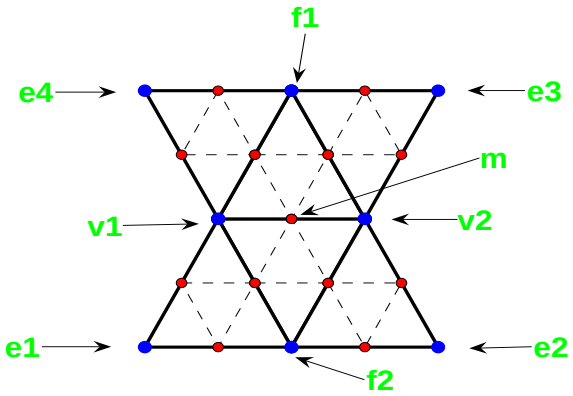

Analysis(j) :

$$\forall m \in \mathcal{M}^j : d_m^j = c_m^{j+1} - \sum_{k \in \mathcal{K}_m} \tilde{s}_{k,m}^j c_k^j,$$

$$\forall m \in \mathcal{K}^j : c_k^j = c_k^{j+1}.$$

Synthesis(j) :

$$\forall m \in \mathcal{K}^j : c_k^j = c_k^j,$$

$$\forall m \in \mathcal{M}^j : c_m^{j+1} = d_m^j + \sum_{k \in \mathcal{K}_m} \tilde{s}_{k,m}^j c_k^j.$$

The members of the neighborhoods used in wavelet bases ($m \in \mathcal{M}^j$, $\mathcal{K}_m = \{v_1, v_2, f_1, f_2, e_1, e_2, e_3, e_4\}$).

Fast wavelet transform

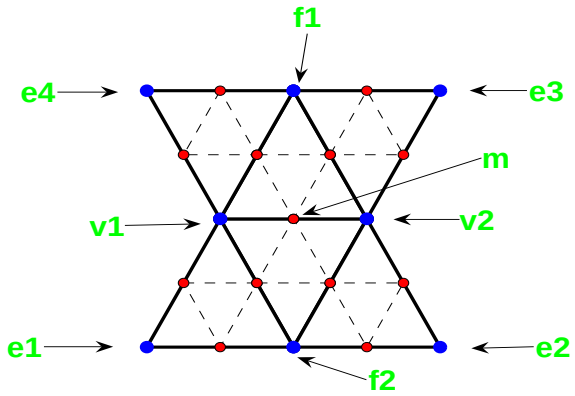

Analysis(j) :

$$\forall m \in \mathcal{M}^j : d_m^j = c_m^{j+1} - \sum_{k \in \mathcal{K}_m} \tilde{s}_{k,m}^j c_k^j,$$

$$\forall m \in \mathcal{K}^j : c_k^j = c_k^{j+1}.$$

Synthesis(j) :

$$\forall m \in \mathcal{K}^j : c_k^j = c_k^j,$$

$$\forall m \in \mathcal{M}^j : c_m^{j+1} = d_m^j + \sum_{k \in \mathcal{K}_m} \tilde{s}_{k,m}^j c_k^j.$$

The members of the neighborhoods used in wavelet bases ($m \in \mathcal{M}^j$, $\mathcal{K}_m = \{v_1, v_2, f_1, f_2, e_1, e_2, e_3, e_4\}$).

For linear basis, $\tilde{s}_{v_1} = \tilde{s}_{v_2} = 1/2$

Fast wavelet transform

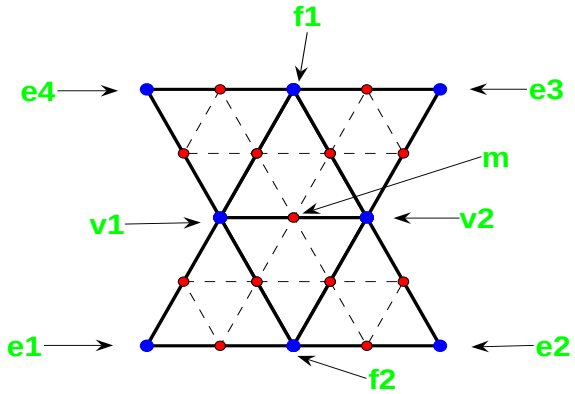

Analysis(j) :

$$\forall m \in \mathcal{M}^j : d_m^j = c_m^{j+1} - \sum_{k \in \mathcal{K}_m} \tilde{s}_{k,m}^j c_k^j,$$

$$\forall m \in \mathcal{K}^j : c_k^j = c_k^{j+1}.$$

Synthesis(j) :

$$\forall m \in \mathcal{K}^j : c_k^j = c_k^j,$$

$$\forall m \in \mathcal{M}^j : c_m^{j+1} = d_m^j + \sum_{k \in \mathcal{K}_m} \tilde{s}_{k,m}^j c_k^j.$$

The members of the neighborhoods used in wavelet bases ($m \in \mathcal{M}^j$, $\mathcal{K}_m = \{v_1, v_2, f_1, f_2, e_1, e_2, e_3, e_4\}$).

For Butterfly basis, $\tilde{s}_{v_1} = \tilde{s}_{v_2} = 1/2$, $\tilde{s}_{f_1} = \tilde{s}_{f_2} = 1/8$, $\tilde{s}_{e_1} = \tilde{s}_{e_2} = \tilde{s}_{e_3} = -1/16$

Fast wavelet transform

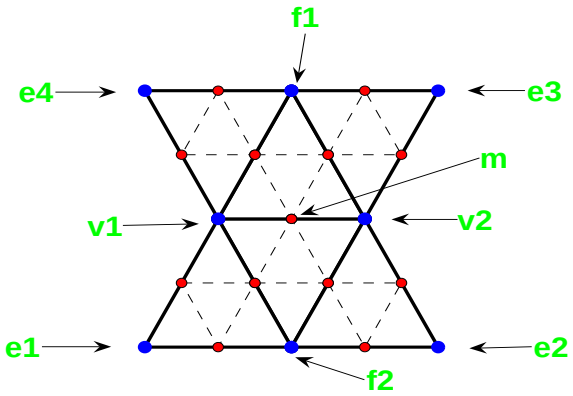

Analysis(j) :

$$\forall m \in \mathcal{M}^j : d_m^j = c_m^{j+1} - \sum_{k \in \mathcal{K}_m} \tilde{s}_{k,m}^j c_k^j,$$

$$\forall m \in \mathcal{M}^j : c_k^j = c_k^{j+1} + s_{k,m}^j d_m^j.$$

Synthesis(j) :

$$\forall m \in \mathcal{M}^j : c_k^j = c_k^j - \sum_{k \in \mathcal{K}_m} s_{k,m}^j d_m^j,$$

$$\forall m \in \mathcal{M}^j : c_m^{j+1} = d_m^j + \sum_{k \in \mathcal{K}_m} \tilde{s}_{k,m}^j c_k^j.$$

The members of the neighborhoods used in wavelet bases ($m \in \mathcal{M}^j$, $\mathcal{K}_m = \{v_1, v_2, f_1, f_2, e_1, e_2, e_3, e_4\}$).

Wavelet compression

$$u^J(p) = \sum_{k \in \mathcal{K}^0} c_k^{J_0} \phi_k^{J_0}(p) + \sum_{j=J_0}^{j=J-1} \sum_{m \in \mathcal{M}^j} d_m^j \psi_m^j(p)$$

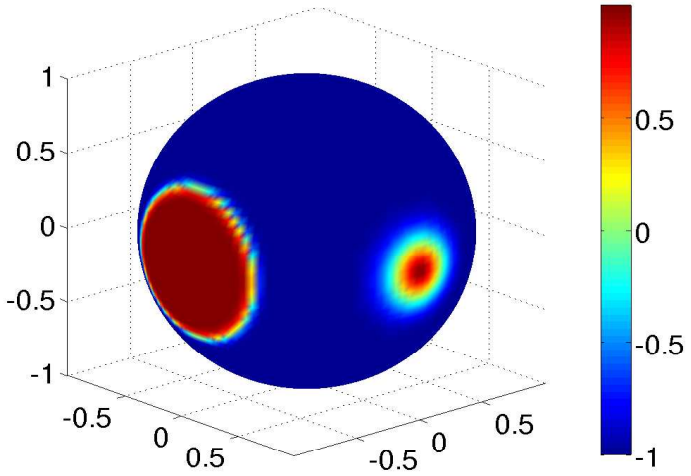

Test function

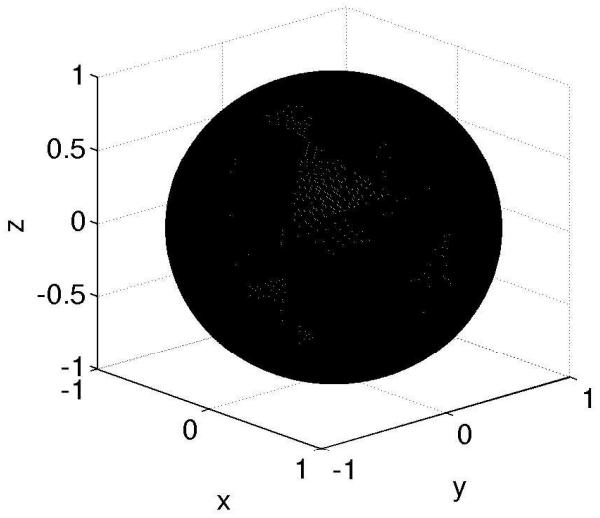

Wavelet locations x_k^J without compression at $J = 6$, $\#\mathcal{K}^6 = 40962$

Wavelet compression

$$u^J_{\geq}(p) = \sum_{k\in\mathcal{K}^0} c_k^{J_0}\phi_k^{J_0}(p) + \sum_{j=J_0}^{j=J-1}\Big(\sum_{\substack{m\in\mathcal{M}^j \\ |d_m^j|\geq\epsilon}} d_m^j\psi_m^j(p) + \sum_{\substack{m\in\mathcal{M}^j \\ |d_m^j|\leq\epsilon}} d_m^j\psi_m^j(p)\Big)$$

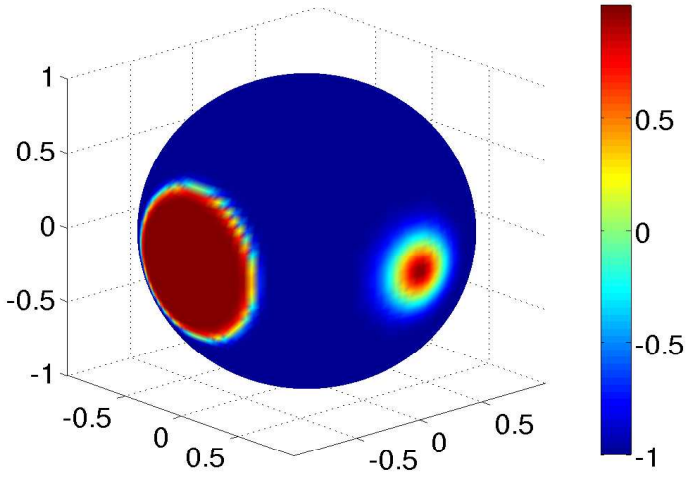

Test function

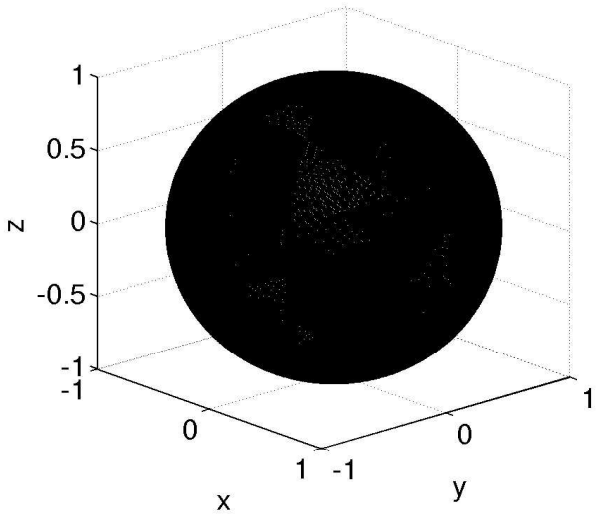

Wavelet locations x_k^J without compression at $J = 6$, $\#\mathcal{K}^6 = 40962$

Wavelet compression

$$u^J_{\geq}(p) = \sum_{k\in\mathcal{K}^0} c^{J_0}_k \phi^{J_0}_k(p) + \sum_{j=J_0}^{j=J-1} \sum_{\substack{m\in\mathcal{M}^j \\ |d^j_m|\geq\epsilon}} d^j_m \psi^j_m(p) + \text{Discarded term}$$

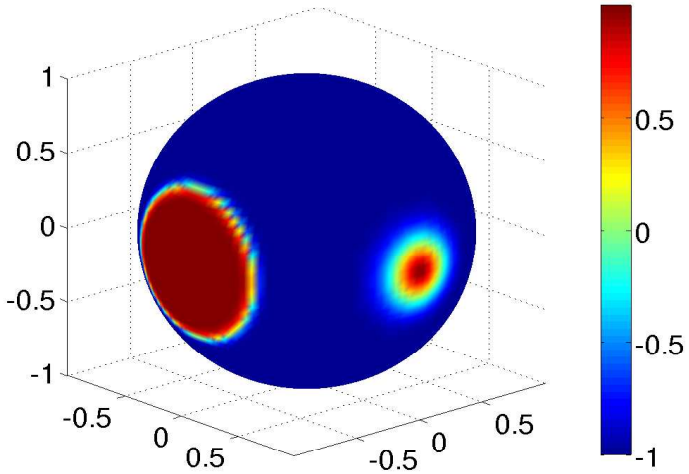

Test function

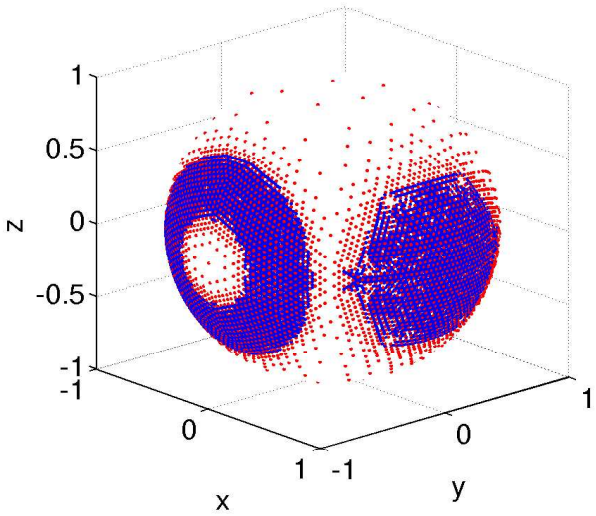

Wavelet locations x^J_k st $J = 6$, $\epsilon = 10^{-5}$, $N(\epsilon) = 8175$ and ratio $\frac{\#\mathcal{K}^6}{N(\epsilon)} \approx 5$

Wavelet compression

$$u^J(p) = \sum_{k \in \mathcal{K}^0} c_k^{J_0} \phi_k^{J_0}(p) + \sum_{j=J_0}^{j=J-1} \sum_{m \in \mathcal{M}^j} d_m^j \psi_m^j(p)$$

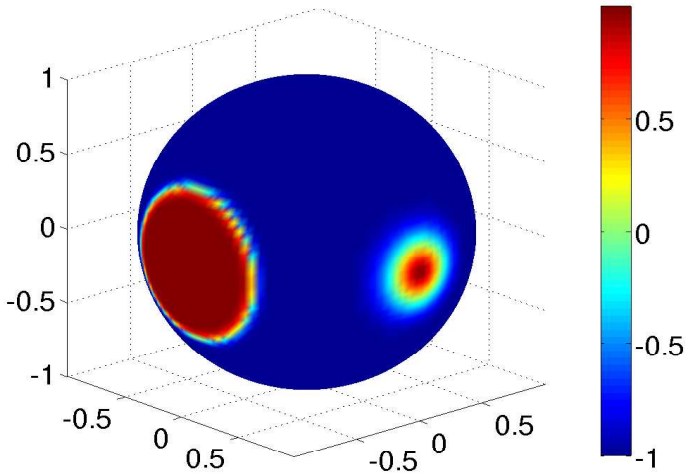

Test function

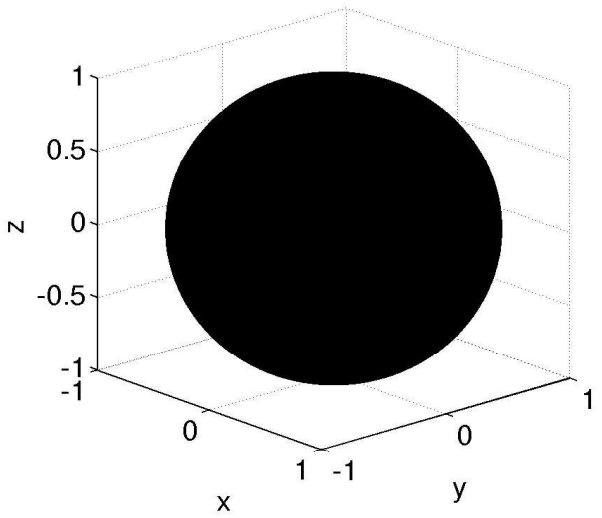

Wavelet locations x_k^J without compression at $J = 7$, $\#\mathcal{K}^7 = 163842$

Wavelet compression

$$u^J_{\geq}(p) = \sum_{k\in\mathcal{K}^0} c^{J_0}_k \phi^{J_0}_k(p) + \sum_{j=J_0}^{j=J-1} \sum_{\substack{m\in\mathcal{M}^j \\ |d^j_m|\geq\epsilon}} d^j_m \psi^j_m(p) + \text{Discarded term}$$

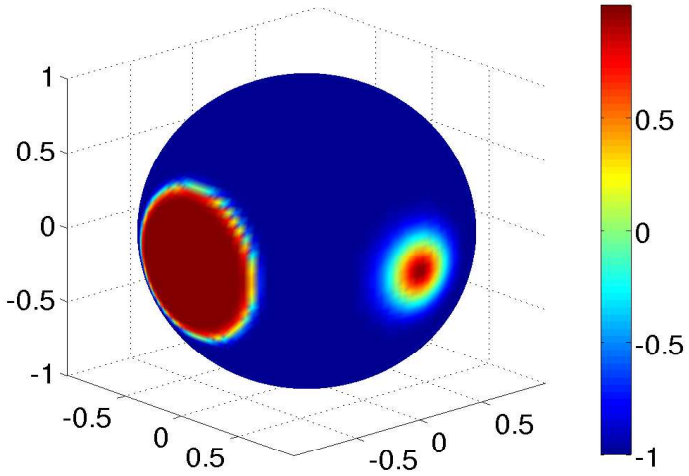

Test function

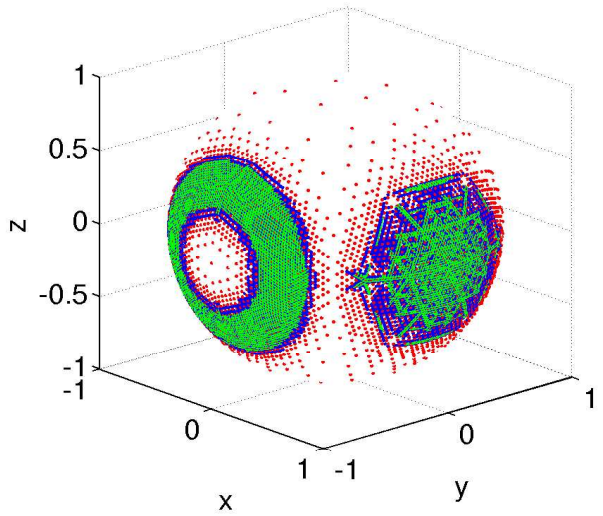

Wavelet locations x^J_k at $J = 7$, $\epsilon = 10^{-5}$, $N(\epsilon) = 20353$ and ratio $\frac{\#\mathcal{K}^7}{N(\epsilon)} \approx 8$

Wavelet compression

$$u^J(p) = \sum_{k \in \mathcal{K}^0} c_k^{J_0} \phi_k^{J_0}(p) + \sum_{j=J_0}^{j=J-1} \sum_{m \in \mathcal{M}^j} d_m^j \psi_m^j(p)$$

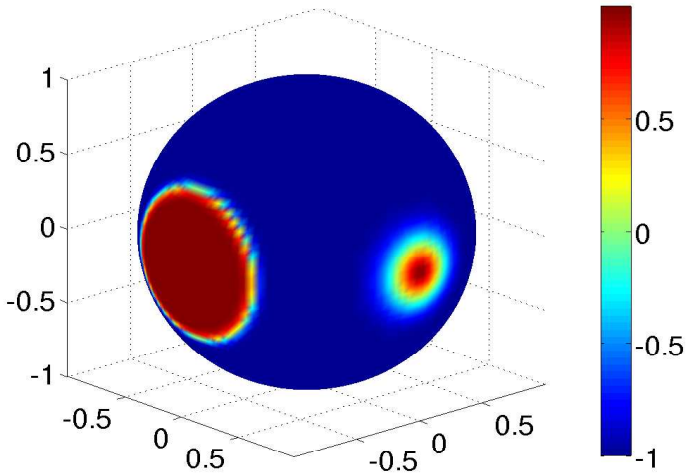

Test function

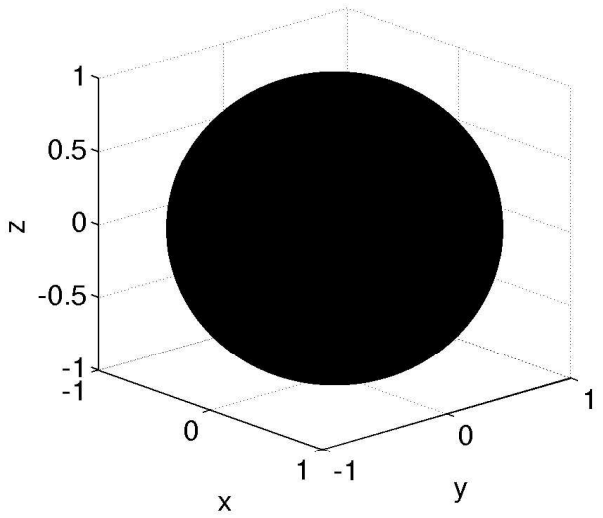

Wavelet locations x_k^J without compression at $J = 8$, $\#\mathcal{K}^8 = 655362$

Wavelet compression

$$u^J_{\geq}(p) = \sum_{k\in\mathcal{K}^0} c^{J_0}_k \phi^{J_0}_k(p) + \sum_{j=J_0}^{j=J-1} \sum_{\substack{m\in\mathcal{M}^j \\ |d^j_m|\geq\epsilon}} d^j_m \psi^j_m(p) + \text{Discarded term}$$

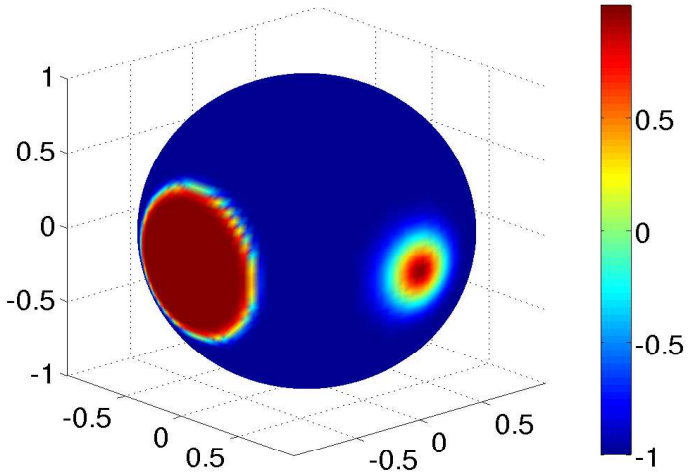

Test function

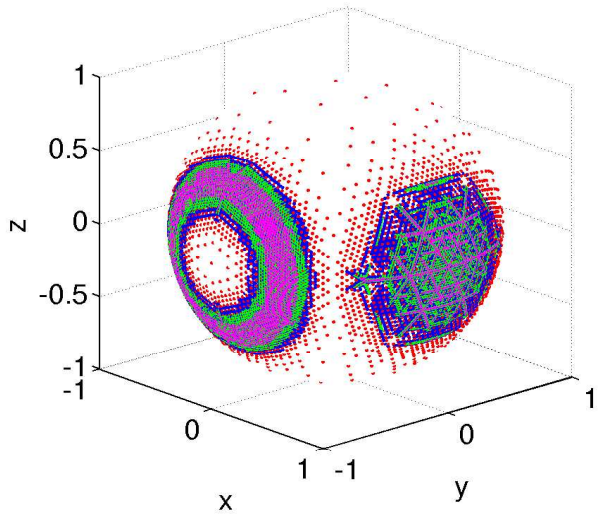

Wavelet locations x^J_k at $J = 8$, $\epsilon = 10^{-5}$, $N(\epsilon) = 64231$ and ratio $\frac{\#\mathcal{K}^8}{N(\epsilon)} \approx 10$

Wavelet approximation estimates

- ϵ controls the total active grid points $N(\epsilon)$ by the following relation $N(\epsilon) \leq c_2 \epsilon^{-\frac{n}{d}}$
- Therefore, approximation error is controlled by active grid points $||u^J(p) - u^J_{\geq}(p)||_\infty \leq c_3 N(\epsilon)^{-\frac{d}{n}}$

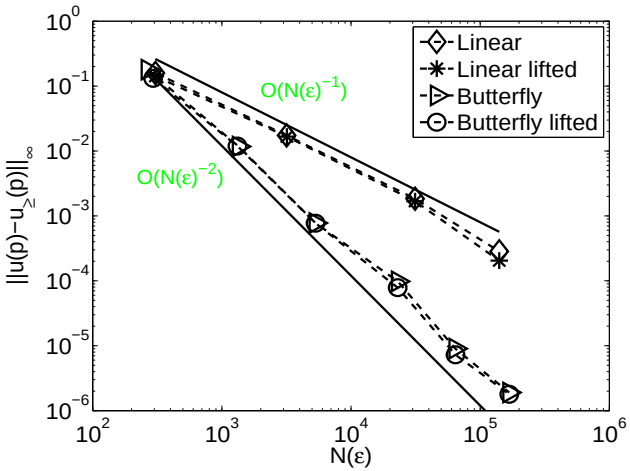

Wavelet approximation estimates

- Approximation error is controlled by the wavelet threshold ϵ

$$||u^J(p) - u^J_{\geq}(p)||_\infty \leq c_1 \epsilon$$

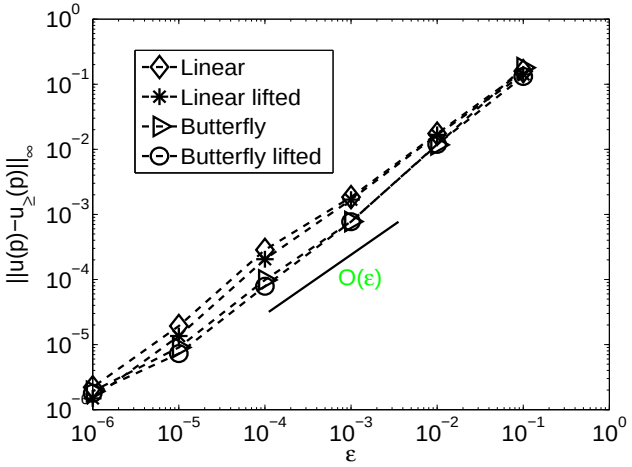

Ref: M. Mehra, N.K.-R. Kevlahan, An adaptive wavelet collocation method for the solution of partial differential equations on the sphere, Under the revision in **J. Comp. Phys.** Available at `www.math.mcmaster.ca/kevla/pdf/articles/sphere_wlt.pdf`

Calculation of Laplace-Beltrami operator on adaptive grid

$$\Delta_{\mathcal{S}} u(p_i^j) = \frac{1}{A_{\mathcal{S}}(p_i^j)} \sum_{k \in N(i)} \frac{\cot \alpha_{i,k} + \cot \beta_{i,k}}{2} [u(p_k^j) - u(p_i^j)]$$

where $A_{\mathcal{S}}(p_i^j)$ is the area of one-ring neighborhood region given by $A_{\mathcal{S}}(p_i^j) = \frac{1}{8} \sum_{k \in N(i)} (\cot \alpha_{i,k} + \cot \beta_{i,k}) \| p_k^j - p_i^j \|^2$.

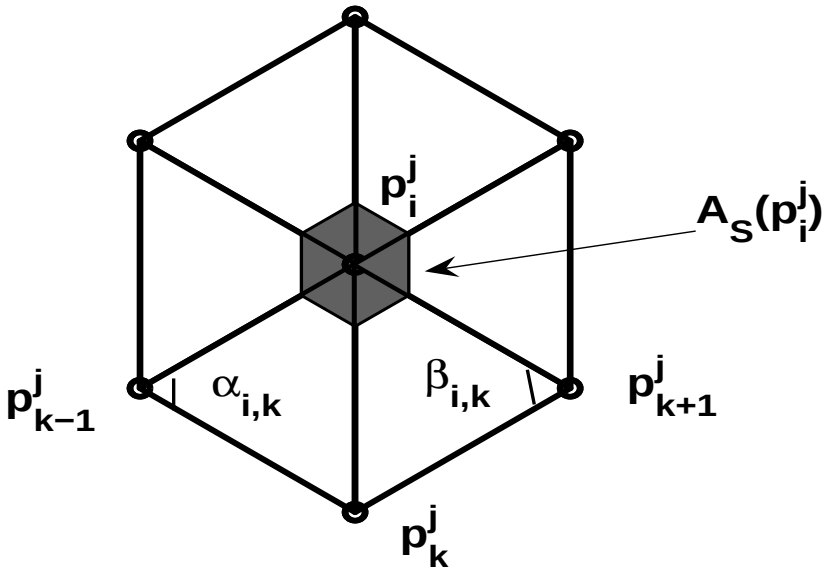

Calculation of Laplace-Beltrami operator on adaptive grid

$$\Delta_S u(p_i^j) = \frac{1}{A_S(p_i^j)} \sum_{k \in N(i)} \frac{\cot \alpha_{i,k} + \cot \beta_{i,k}}{2} [u(p_k^j) - u(p_i^j)]$$

- Convergence result for the Laplace-Beltrami operator of $u_{\geq}^J(p)$

$$||\Delta_S u^J(p) - \Delta_S u_{\geq}^J(p)||_\infty \leq c_4 \epsilon$$

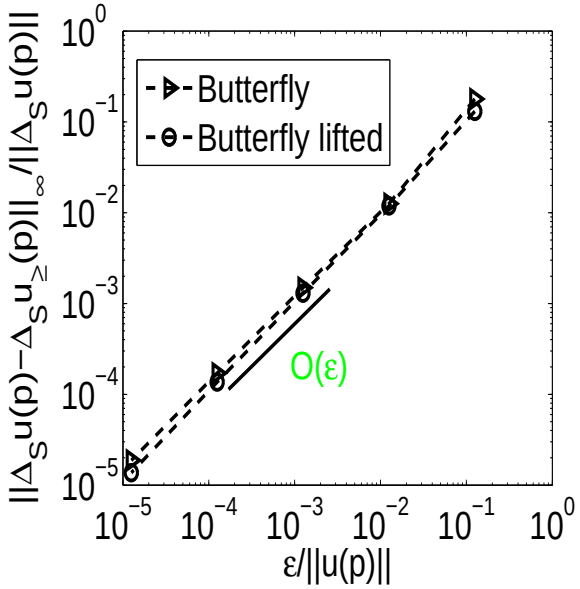

Calculation of Laplace-Beltrami operator on adaptive grid

$$\Delta_S u(p_i^j) = \frac{1}{A_S(p_i^j)} \sum_{k \in N(i)} \frac{\cot \alpha_{i,k} + \cot \beta_{i,k}}{2} [u(p_k^j) - u(p_i^j)]$$

- Convergence result for the Laplace-Beltrami operator of $u_{\geq}^J(p)$

$$||\Delta_S u^J(p) - \Delta_S u_{\geq}^J(p)||_\infty \leq c_4 \epsilon$$
$$\leq c_5 N(\epsilon)^{-\frac{d-2}{n}}$$

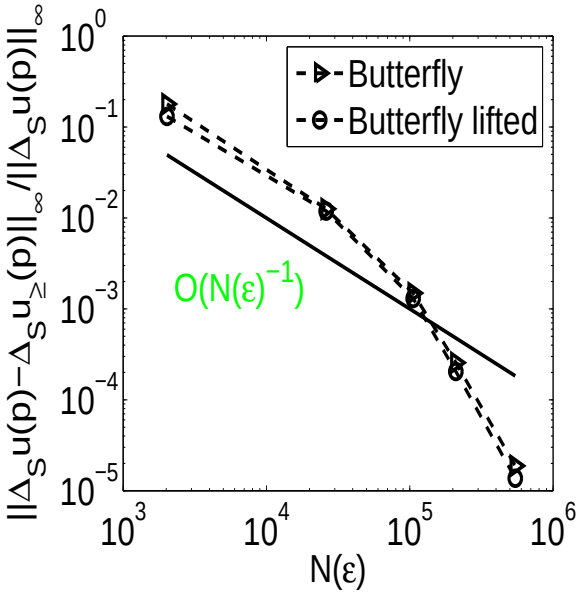

Calculation of other differential operators on adaptive grid

- The flux term present in the spherical advection equation can be expressed in the form of flux divergence and Jacobian operators, $\nabla.(Vu) = \nabla.(u\nabla\chi) - J(u,\psi)$
- $J_S(u(p_i^j),\psi(p_i^j)) = \frac{1}{6A_S(p_i^j)}\sum_{k\in N(i)}(u(p_k^j)+u(p_i^j))(\psi(p_k^j)-\psi(p_i^j))$
- $$\nabla_S.(u(p_i^j),\nabla_S\chi(p_i^j)) = \frac{1}{2A_S(p_i^j)}\sum_{k\in N(i)}\frac{\cot\alpha_{i,k}+\cot\beta_{i,k}}{2}$$
$$(u(p_k^j)+u(p_i^j))(\psi(p_k^j)-\psi(p_i^j)).$$

Calculation of other differential operators on adaptive grid

- The flux term present in the spherical advection equation can be expressed in the form of flux divergence and Jacobian operators, $\nabla.(Vu) = \nabla.(u\nabla\chi) - J(u,\psi)$
- $J_S(u(p_i^j),\psi(p_i^j)) = \frac{1}{6A_S(p_i^j)}\sum_{k\in N(i)}(u(p_k^j)+u(p_i^j))(\psi(p_k^j)-\psi(p_i^j))$
-

$$\nabla_S.(u(p_i^j),\nabla_S\chi(p_i^j)) = \frac{1}{2A_S(p_i^j)}\sum_{k\in N(i)}\frac{\cot\alpha_{i,k}+\cot\beta_{i,k}}{2}$$
$$(u(p_k^j)+u(p_i^j))(\psi(p_k^j)-\psi(p_i^j)).$$

Calculation of other differential operators on adaptive grid

- The flux term present in the spherical advection equation can be expressed in the form of flux divergence and Jacobian operators, $\nabla.(Vu) = \nabla.(u\nabla\chi) - J(u,\psi)$
- $J_{\mathcal{S}}(u(p_i^j),\psi(p_i^j)) = \frac{1}{6A_{\mathcal{S}}(p_i^j)}\sum_{k\in N(i)}(u(p_k^j)+u(p_i^j))(\psi(p_k^j)-\psi(p_i^j))$
-

$$\nabla_{\mathcal{S}}.(u(p_i^j),\nabla_{\mathcal{S}}\chi(p_i^j)) = \frac{1}{2A_{\mathcal{S}}(p_i^j)}\sum_{k\in N(i)}\frac{\cot\alpha_{i,k}+\cot\beta_{i,k}}{2}$$
$$(u(p_k^j)+u(p_i^j))(\psi(p_k^j)-\psi(p_i^j)).$$

Application of spherical wavelets to compress turbulence

- What is turbulence?
  - Smooth flow is not possible at $Re = \frac{uL}{\nu} >> 1$, and at $Re = O(10^4)$ it becomes turbulent.
  - In direct numerical simulation (DNS) we compute all degrees of freedom of the flow, whose number increases with Reynolds number (e.g N(total number of grid points) $\approx Re$ for two–dimensional DNS and $N \approx Re^{9/4}$ for three–dimensional DNS). Atmospherical flows have $Re \geq 10^6$, therefore, **the computation of atmospheric flows remain a grand challenge!!**
- What are coherent structures?
  - A coherent structure is associated with motion of collective part of fluid (e.g in geophysical fluid dynamics many of coherent structures are vortices (local masses of rapidly rotation fluid))
  - We find vortices on all scales, from little dust devils on a hot summer day to ocean eddies thousand kilometer across

Application of spherical wavelets to compress turbulence

- What is turbulence?
  - Smooth flow is not possible at $Re = \frac{uL}{\nu} >> 1$, and at $Re = O(10^4)$ it becomes turbulent.
  - In direct numerical simulation (DNS) we compute all degrees of freedom of the flow, whose number increases with Reynolds number (e.g N(total number of grid points) $\approx Re$ for two–dimensional DNS and $N \approx Re^{9/4}$ for three–dimensional DNS). Atmospherical flows have $Re \geq 10^6$, therefore, **the computation of atmospheric flows remain a grand challenge!!**
- What are coherent structures?
  - A coherent structure is associated with motion of collective part of fluid (e.g in geophysical fluid dynamics many of coherent structures are vortices (local masses of rapidly rotation fluid))
  - We find vortices on all scales, from little dust devils on a hot summer day to ocean eddies thousand kilometer across

Application of spherical wavelets to compress turbulence

- What is turbulence?
  - Smooth flow is not possible at $Re = \frac{uL}{\nu} >> 1$, and at $Re = O(10^4)$ it becomes turbulent.
  - In direct numerical simulation (DNS) we compute all degrees of freedom of the flow, whose number increases with Reynolds number (e.g N(total number of grid points) $\approx Re$ for two–dimensional DNS and $N \approx Re^{9/4}$ for three–dimensional DNS). Atmospherical flows have $Re \geq 10^6$, therefore, **the computation of atmospheric flows remain a grand challenge!!**
- What are coherent structures?
  - A coherent structure is associated with motion of collective part of fluid (e.g in geophysical fluid dynamics many of coherent structures are vortices (local masses of rapidly rotation fluid))
  - We find vortices on all scales, from little dust devils on a hot summer day to ocean eddies thousand kilometer across

Application of spherical wavelets to compress turbulence

- What is turbulence?
  - Smooth flow is not possible at $Re = \frac{uL}{\nu} >> 1$, and at $Re = O(10^4)$ it becomes turbulent.
  - In direct numerical simulation (DNS) we compute all degrees of freedom of the flow, whose number increases with Reynolds number (e.g N(total number of grid points) $\approx Re$ for two–dimensional DNS and $N \approx Re^{9/4}$ for three–dimensional DNS). Atmospherical flows have $Re \geq 10^6$, therefore, **the computation of atmospheric flows remain a grand challenge!!**
- What are coherent structures?
  - A coherent structure is associated with motion of collective part of fluid (e.g in geophysical fluid dynamics many of coherent structures are vortices (local masses of rapidly rotation fluid))
  - We find vortices on all scales, from little dust devils on a hot summer day to ocean eddies thousand kilometer across

Application of spherical wavelets to compress turbulence

- What is turbulence?
  - Smooth flow is not possible at $Re = \frac{uL}{\nu} >> 1$, and at $Re = O(10^4)$ it becomes turbulent.
  - In direct numerical simulation (DNS) we compute all degrees of freedom of the flow, whose number increases with Reynolds number (e.g N(total number of grid points) $\approx Re$ for two–dimensional DNS and $N \approx Re^{9/4}$ for three–dimensional DNS). Atmospherical flows have $Re \geq 10^6$, therefore, **the computation of atmospheric flows remain a grand challenge!!**
- What are coherent structures?
  - A coherent structure is associated with motion of collective part of fluid (e.g in geophysical fluid dynamics many of coherent structures are vortices (local masses of rapidly rotation fluid))
  - We find vortices on all scales, from little dust devils on a hot summer day to ocean eddies thousand kilometer across

Application of spherical wavelets to compress turbulence

- What is turbulence?
  - Smooth flow is not possible at $Re = \frac{uL}{\nu} >> 1$, and at $Re = O(10^4)$ it becomes turbulent.
  - In direct numerical simulation (DNS) we compute all degrees of freedom of the flow, whose number increases with Reynolds number (e.g N(total number of grid points) $\approx Re$ for two–dimensional DNS and $N \approx Re^{9/4}$ for three–dimensional DNS). Atmospherical flows have $Re \geq 10^6$, therefore, **the computation of atmospheric flows remain a grand challenge!!**
- What are coherent structures?
  - A coherent structure is associated with motion of collective part of fluid (e.g in geophysical fluid dynamics many of coherent structures are vortices (local masses of rapidly rotation fluid))
  - We find vortices on all scales, from little dust devils on a hot summer day to ocean eddies thousand kilometer across

Application of spherical wavelets to compress turbulence

- What is turbulence?
  - Smooth flow is not possible at $Re = \frac{uL}{\nu} >> 1$, and at $Re = O(10^4)$ it becomes turbulent.
  - In direct numerical simulation (DNS) we compute all degrees of freedom of the flow, whose number increases with Reynolds number (e.g N(total number of grid points) $\approx Re$ for two–dimensional DNS and $N \approx Re^{9/4}$ for three–dimensional DNS). Atmospherical flows have $Re \geq 10^6$, therefore, **the computation of atmospheric flows remain a grand challenge!!**
- What are coherent structures?
  - A coherent structure is associated with motion of collective part of fluid (e.g in geophysical fluid dynamics many of coherent structures are vortices (local masses of rapidly rotation fluid))
  - We find vortices on all scales, from little dust devils on a hot summer day to ocean eddies thousand kilometer across

Application of spherical wavelets to compress turbulence

- Turbulence can be divided into two orthogonal parts: a organized (coherent), inhomogeneous, non-Gaussian component and random noise (incoherent), homogeneous and Gaussian component.
- The coherent vortices must be resolved, but the noise may be modeled (or neglected entirely).
- The coherent vortices can be extracted using nonlinear wavelet filtering.

This is the concept of Coherent Vortex Simulation which was developed by Marie Farge, Kai Schneider and Nicholas Kevlahan in flat geometries.

Application of spherical wavelets to compress turbulence

- Turbulence can be divided into two orthogonal parts: a organized (coherent), inhomogeneous, non-Gaussian component and random noise (incoherent), homogeneous and Gaussian component.
- The coherent vortices must be resolved, but the noise may be modeled (or neglected entirely).
- The coherent vortices can be extracted using nonlinear wavelet filtering.

This is the concept of Coherent Vortex Simulation which was developed by Marie Farge, Kai Schneider and Nicholas Kevlahan in flat geometries.

Application of spherical wavelets to compress turbulence

- Turbulence can be divided into two orthogonal parts: a organized (coherent), inhomogeneous, non-Gaussian component and random noise (incoherent), homogeneous and Gaussian component.
- The coherent vortices must be resolved, but the noise may be modeled (or neglected entirely).
- The coherent vortices can be extracted using nonlinear wavelet filtering.

This is the concept of Coherent Vortex Simulation which was developed by Marie Farge, Kai Schneider and Nicholas Kevlahan in flat geometries.

Application of spherical wavelets to compress turbulence

- Turbulence can be divided into two orthogonal parts: a organized (coherent), inhomogeneous, non-Gaussian component and random noise (incoherent), homogeneous and Gaussian component.
- The coherent vortices must be resolved, but the noise may be modeled (or neglected entirely).
- The coherent vortices can be extracted using nonlinear wavelet filtering.

This is the concept of Coherent Vortex Simulation which was developed by Marie Farge, Kai Schneider and Nicholas Kevlahan in flat geometries.

Application of spherical wavelets to compress turbulence

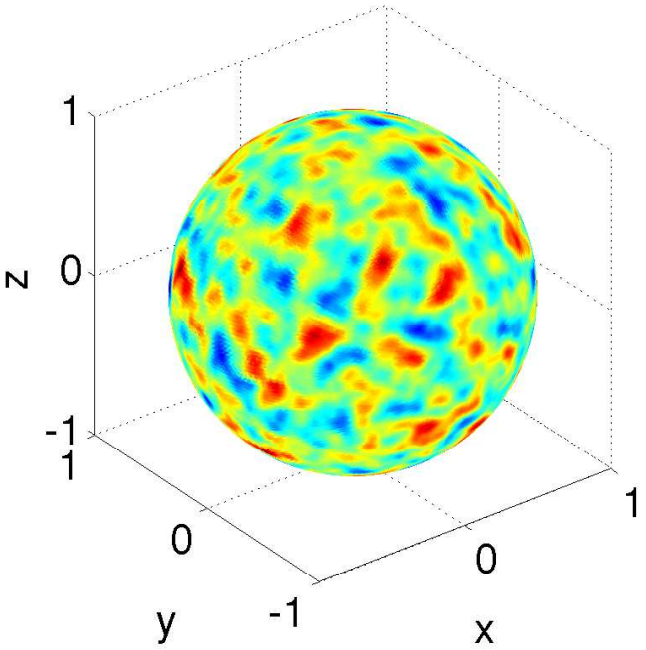

Vorticity function.

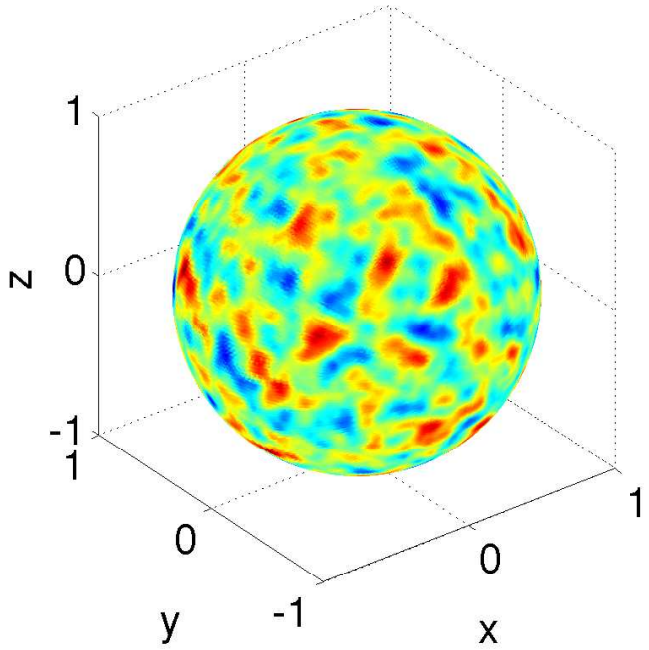

Reconstructed with 40% significant wavelets.

Application of spherical wavelets to compress turbulence

$$E(n,0) = \frac{\mathcal{A} n^{\gamma/2}}{(n+n_0)^{\gamma}}$$

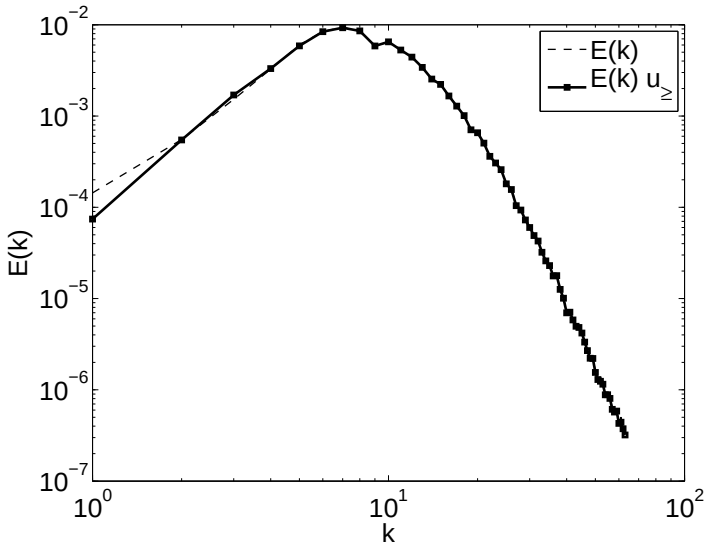

Energy spectrum reconstructed with 40% significant wavelets.

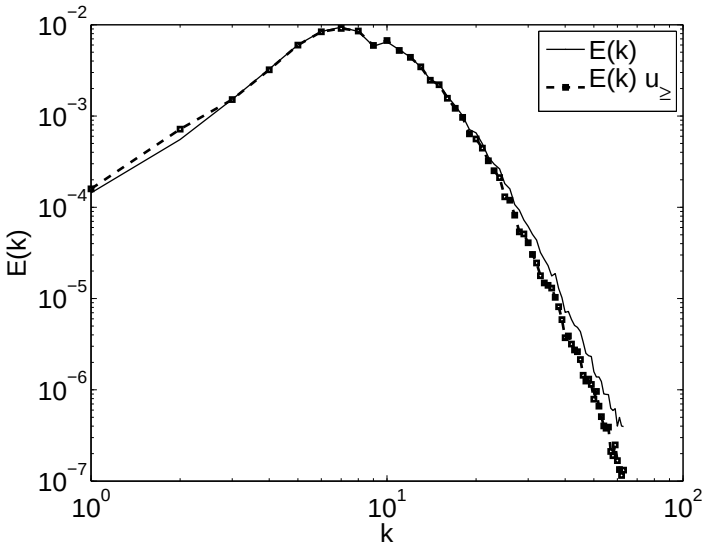

Energy spectrum reconstructed with 2% significant wavelets

Application of spherical wavelets to compress turbulence

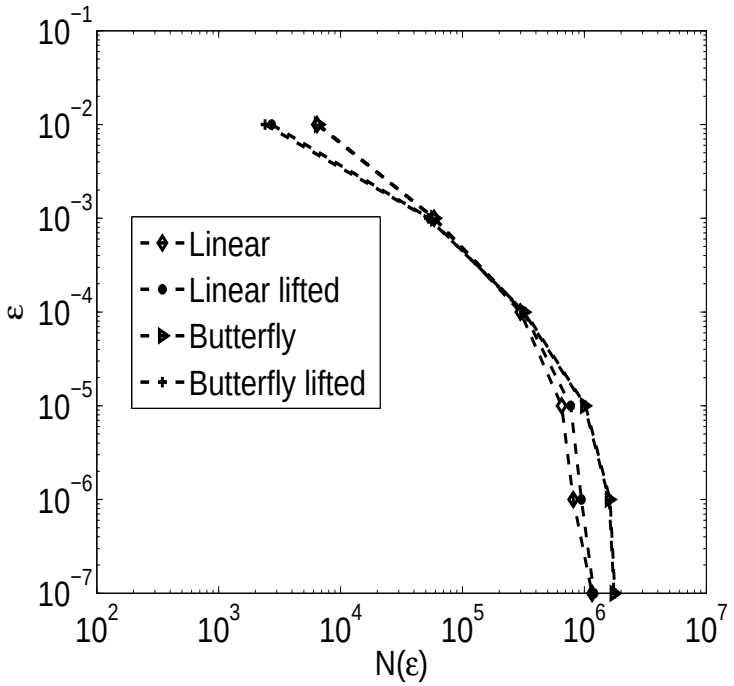

Relation between ϵ and $N(\epsilon)$ for the vorticity function.

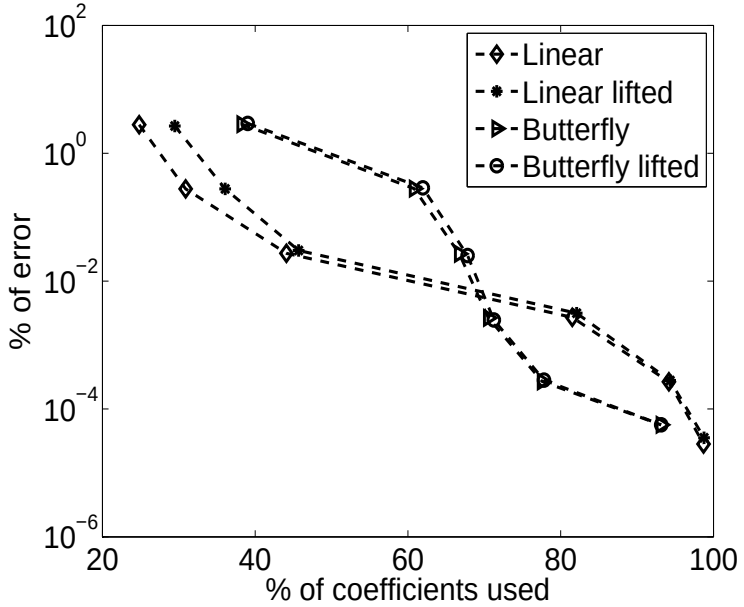

Rate of relative error as a function of rate of significant wavelets $= \frac{N(\epsilon) \times 100}{N(\epsilon=0)}$.

Diffusion equation

$$u_t = \nu \Delta_S u + f$$

where f is localized source chosen such a way that the solution of diffusion equation is given by

$$u(\theta, \phi, t) = 2e^{-\frac{(\theta-\theta_0)^2+(\phi-\phi_0)^2}{\nu(t+1)}}$$

Such equations arise in the application of Willmore flow, surface diffusion flow etc.

Diffusion Equation

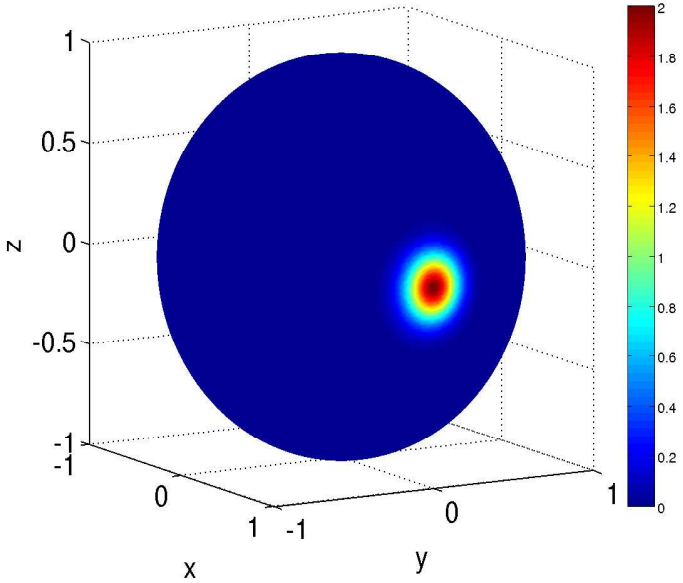

Initial condition at $t = 0$

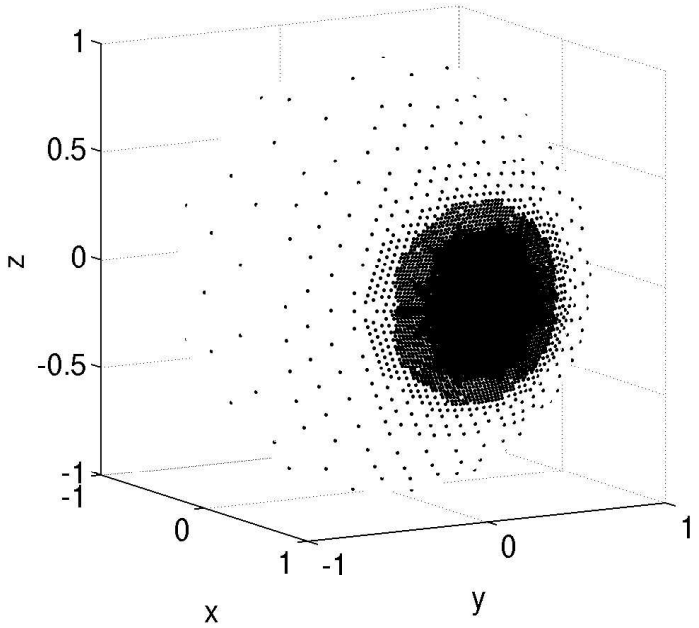

Adaptive grid at $t = 0$

Diffusion Equation

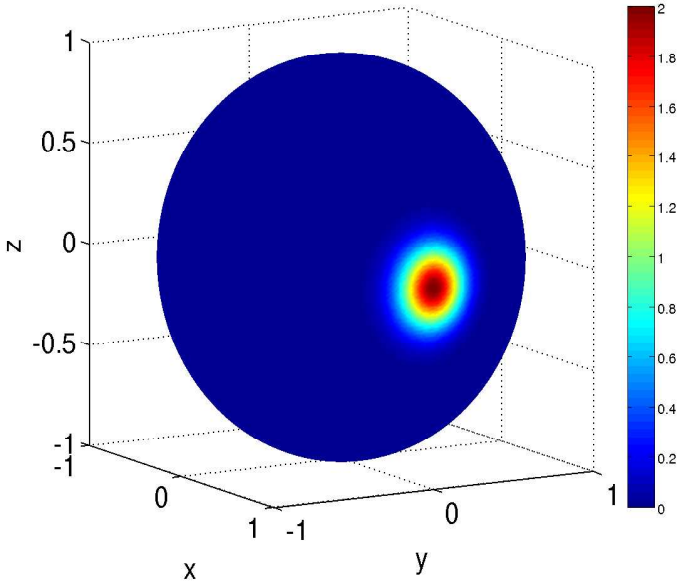

Solution using AWCM at $t = 0.5$

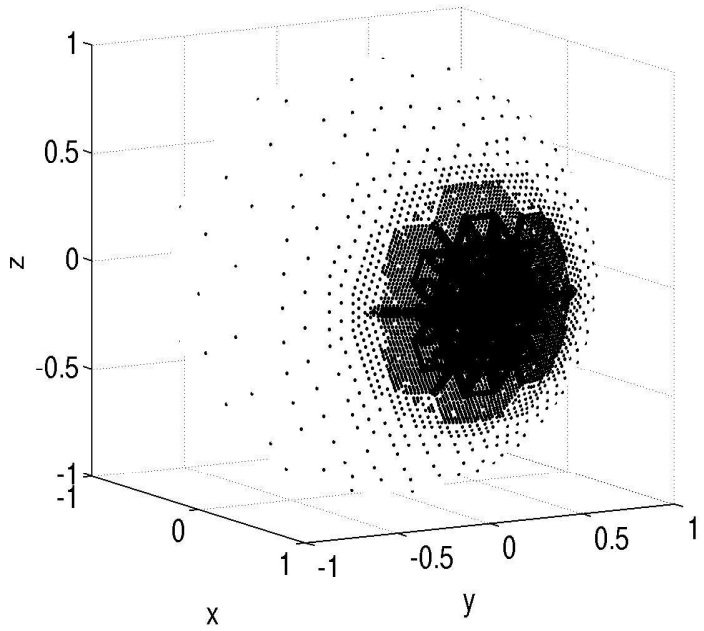

Adaptive grid at $t = 0.5$

Diffusion Equation

The potential of adaptive algorithm is measured by compression coefficients

$$\mathcal{C} = \frac{N(\epsilon = 0)}{N(\epsilon)}$$

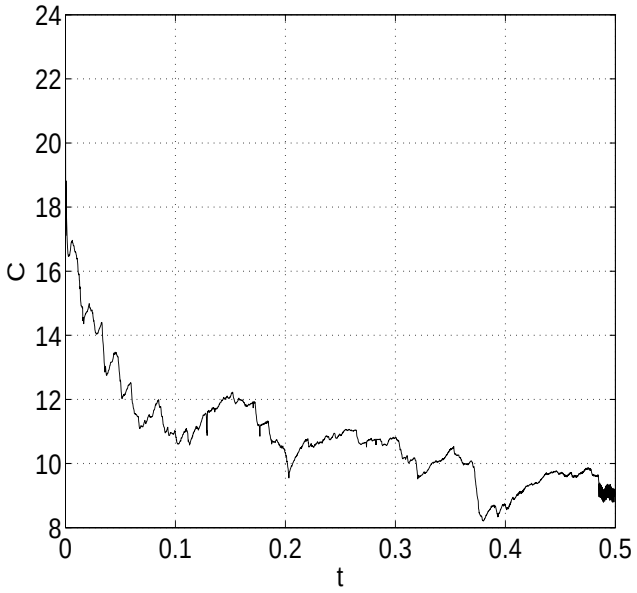

The compression coefficient $\mathcal{C}$ as a function of time, $\epsilon = 10^{-5}$.

Spherical advection equation

$$\frac{\partial u}{\partial t} + V.\nabla_S u = 0,$$

Such equations arise typically in the context of numerical weather forecast or in climatological studies, and they provide some of the most challenging and CPU time consuming problems in modern computational fluid dynamics.

Spherical advection equation

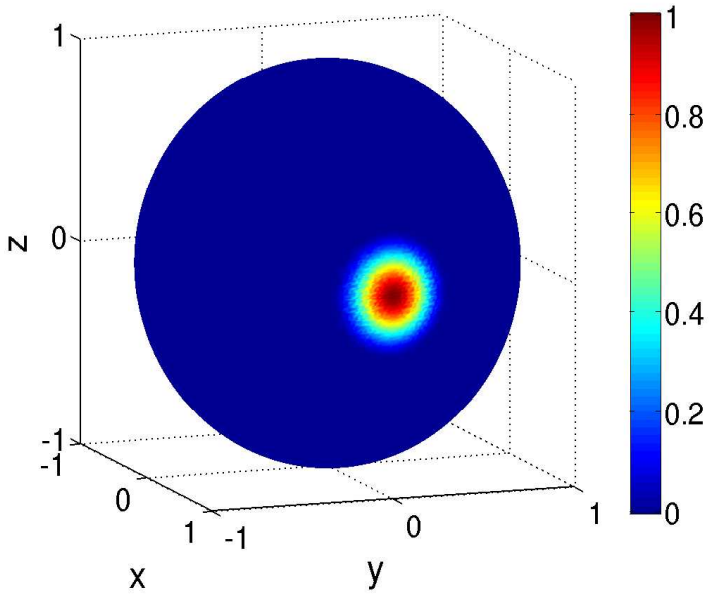

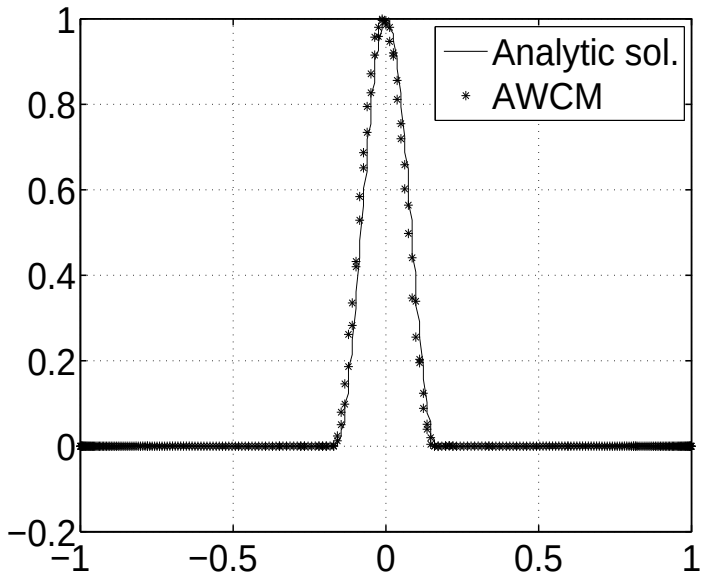

Solid body rotation of cosine bell using AWCM for $\epsilon = 10^{-5}$.

Spherical advection equation

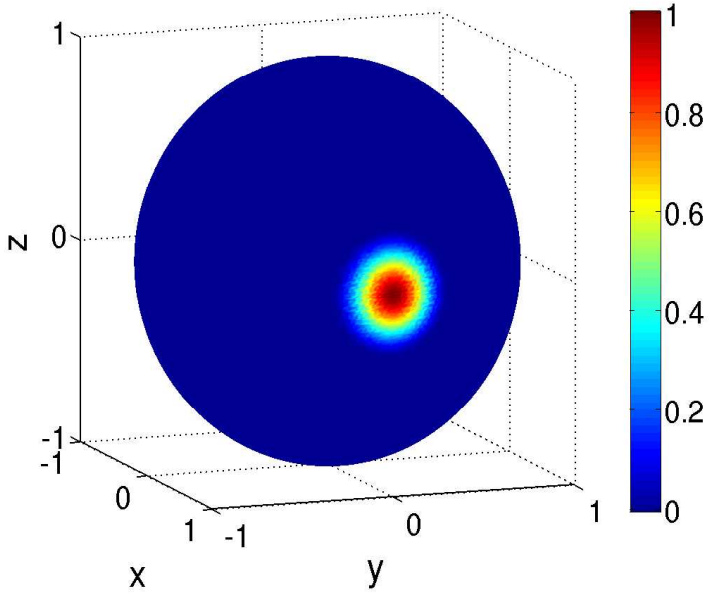

Solution using AWCM

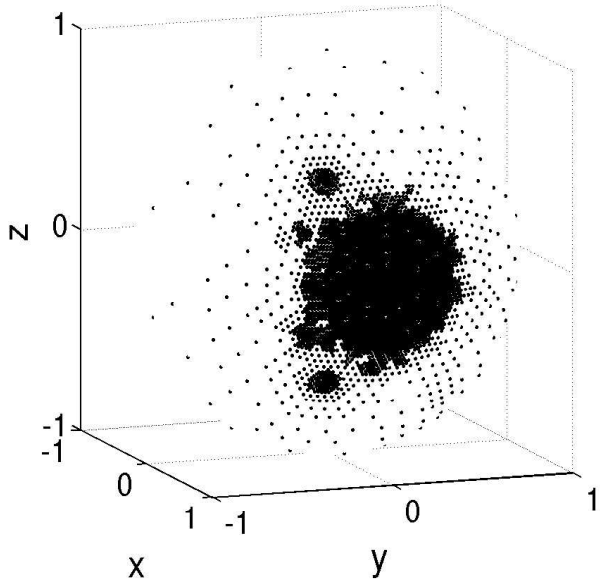

Adapted grid for the solution.

Poisson Equation

Grids

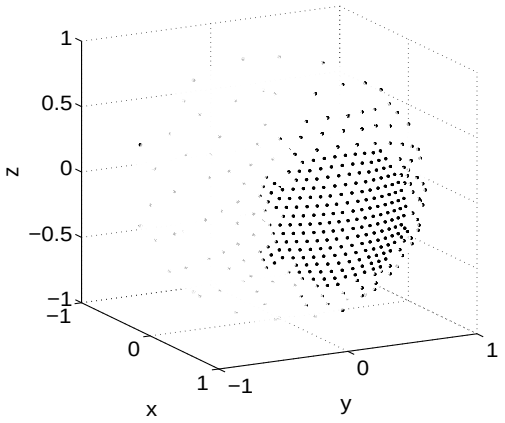

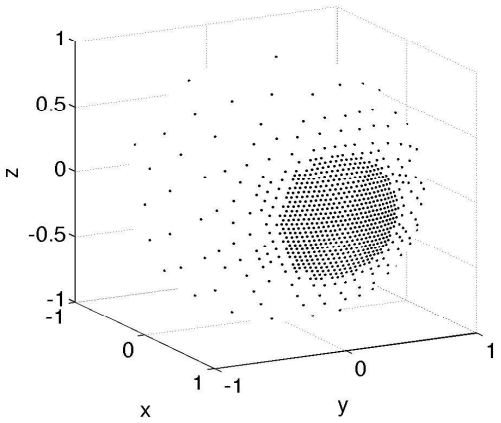

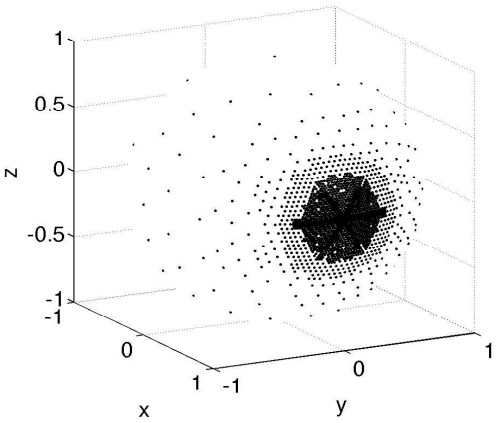

Solutions

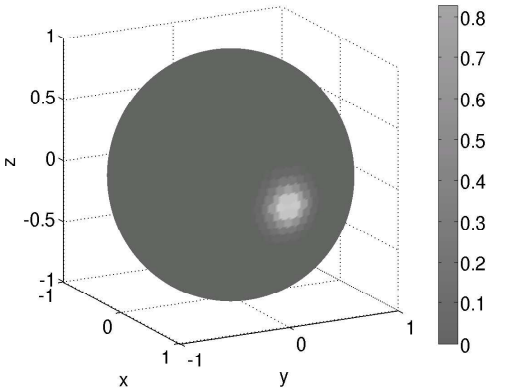

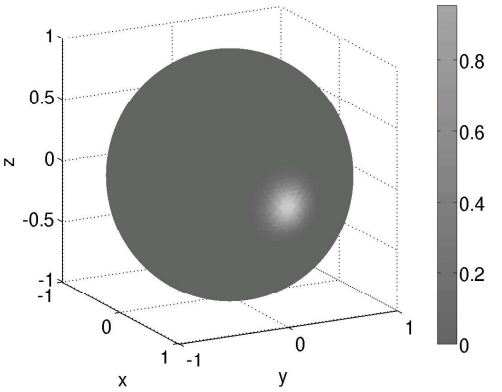

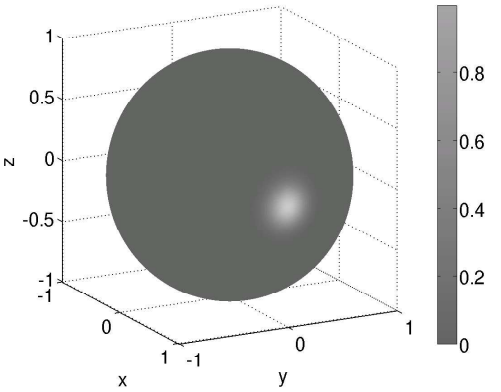

m=5 m=7 m=9

Poisson Equation

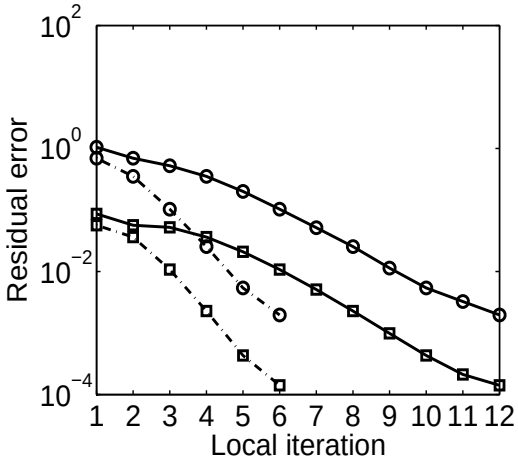

Residual error for threshold $\epsilon = 10^{-4}$ and different choice of smoothing parameters ν_1 and ν_2, $-\circ$ (L_∞ norm, $\nu_1 = \nu_2 = 2$), $-\cdot\circ$ (L_∞ norm, $\nu_1 = \nu_2 = 4$), $-\square$ (L_2 norm, $\nu_1 = \nu_2 = 2$), $-\cdot\square$ (L_2 norm, $\nu_1 = \nu_2 = 4$)

Ref: M. Mehra, N.K.-R. Kevlahan, An adaptive multilevel wavelet solver for elliptic equations on an optimal spherical geodesic grid, Submitted to **SIAM J. Sci. Comp.** (2007). Available at `www.math.mcmaster.ca/kevla/pdf/articles/sphere_mg.pdf`

Conclusions

Adaptive wavelet collocation method:

- Used for time evolution problems (e.g diffusion and advection equations)
- Dynamic adaptivity is necessary for atmospheric modeling.
- Fast $O(\mathcal{N})$ wavelet transform and $O(\mathcal{N})$ hierarchical finite difference schemes over triangulated surface for the differential operators is used.
- Verified convergence result predicted in theory.

Adaptive multilevel wavelet solver:

- Used for elliptic problems (e.g Poisson equation).
- The improved truncation error and efficiency of solver on an optimal spherical geodesic grid

Conclusions

Adaptive wavelet collocation method:

- Used for time evolution problems (e.g diffusion and advection equations)
- Dynamic adaptivity is necessary for atmospheric modeling.
- Fast $O(\mathcal{N})$ wavelet transform and $O(\mathcal{N})$ hierarchical finite difference schemes over triangulated surface for the differential operators is used.
- Verified convergence result predicted in theory.

Adaptive multilevel wavelet solver:

- Used for elliptic problems (e.g Poisson equation).
- The improved truncation error and efficiency of solver on an optimal spherical geodesic grid

Conclusions

Adaptive wavelet collocation method:

- Used for time evolution problems (e.g diffusion and advection equations)
- Dynamic adaptivity is necessary for atmospheric modeling.
- Fast $O(\mathcal{N})$ wavelet transform and $O(\mathcal{N})$ hierarchical finite difference schemes over triangulated surface for the differential operators is used.
- Verified convergence result predicted in theory.

Adaptive multilevel wavelet solver:

- Used for elliptic problems (e.g Poisson equation).
- The improved truncation error and efficiency of solver on an optimal spherical geodesic grid

Conclusions

Adaptive wavelet collocation method:

- Used for time evolution problems (e.g diffusion and advection equations)
- Dynamic adaptivity is necessary for atmospheric modeling.
- Fast $O(\mathcal{N})$ wavelet transform and $O(\mathcal{N})$ hierarchical finite difference schemes over triangulated surface for the differential operators is used.
- Verified convergence result predicted in theory.

Adaptive multilevel wavelet solver:

- Used for elliptic problems (e.g Poisson equation).
- The improved truncation error and efficiency of solver on an optimal spherical geodesic grid

Conclusions

Adaptive wavelet collocation method:

- Used for time evolution problems (e.g diffusion and advection equations)
- Dynamic adaptivity is necessary for atmospheric modeling.
- Fast $O(\mathcal{N})$ wavelet transform and $O(\mathcal{N})$ hierarchical finite difference schemes over triangulated surface for the differential operators is used.
- Verified convergence result predicted in theory.

Adaptive multilevel wavelet solver:

- Used for elliptic problems (e.g Poisson equation).
- The improved truncation error and efficiency of solver on an optimal spherical geodesic grid

Conclusions

Adaptive wavelet collocation method:

- Used for time evolution problems (e.g diffusion and advection equations)
- Dynamic adaptivity is necessary for atmospheric modeling.
- Fast $O(\mathcal{N})$ wavelet transform and $O(\mathcal{N})$ hierarchical finite difference schemes over triangulated surface for the differential operators is used.
- Verified convergence result predicted in theory.

Adaptive multilevel wavelet solver:

- Used for elliptic problems (e.g Poisson equation).
- The improved truncation error and efficiency of solver on an optimal spherical geodesic grid

Conclusions

Adaptive wavelet collocation method:

- Used for time evolution problems (e.g diffusion and advection equations)
- Dynamic adaptivity is necessary for atmospheric modeling.
- Fast $O(\mathcal{N})$ wavelet transform and $O(\mathcal{N})$ hierarchical finite difference schemes over triangulated surface for the differential operators is used.
- Verified convergence result predicted in theory.

Adaptive multilevel wavelet solver:

- Used for elliptic problems (e.g Poisson equation).
- The improved truncation error and efficiency of solver on an optimal spherical geodesic grid

Conclusions

Adaptive wavelet collocation method:

- Used for time evolution problems (e.g diffusion and advection equations)
- Dynamic adaptivity is necessary for atmospheric modeling.
- Fast $O(\mathcal{N})$ wavelet transform and $O(\mathcal{N})$ hierarchical finite difference schemes over triangulated surface for the differential operators is used.
- Verified convergence result predicted in theory.

Adaptive multilevel wavelet solver:

- Used for elliptic problems (e.g Poisson equation).
- The improved truncation error and efficiency of solver on an optimal spherical geodesic grid

Future plans

- Application of AWCM and adaptive multilevel solver to more realistic models (e.g. geostropic turbulence which is an unsolved challenging topic according to Ref: D. G. Dritschel, B. Legras, Modelling ocean and atmospheric vortices, **Physics today**, 1993.) (This work is currently underway!!)
- Application of diffusion wavelets to partial differential equations
  Ref: Biorthogonal diffusion wavelets for multiscale representations on manifolds and graphs Proc. SPIE Vol. 5914, 5914M Wavelets XI; Manos Papadakis, Andrew F. Laine, Michael A. Unser; Eds., 2005

Future plans

- Application of AWCM and adaptive multilevel solver to more realistic models (e.g. geostropic turbulence which is an unsolved challenging topic according to Ref: D. G. Dritschel, B. Legras, Modelling ocean and atmospheric vortices, **Physics today**, 1993.) (This work is currently underway!!)
- Application of diffusion wavelets to partial differential equations
  Ref: Biorthogonal diffusion wavelets for multiscale representations on manifolds and graphs Proc. SPIE Vol. 5914, 5914M Wavelets XI; Manos Papadakis, Andrew F. Laine, Michael A. Unser; Eds., 2005

Future plans

- Application of AWCM and adaptive multilevel solver to more realistic models (e.g. geostropic turbulence which is an unsolved challenging topic according to Ref: D. G. Dritschel, B. Legras, Modelling ocean and atmospheric vortices, **Physics today**, 1993.) (This work is currently underway!!)
- Application of diffusion wavelets to partial differential equations
  Ref: Biorthogonal diffusion wavelets for multiscale representations on manifolds and graphs Proc. SPIE Vol. 5914, 5914M Wavelets XI; Manos Papadakis, Andrew F. Laine, Michael A. Unser; Eds., 2005

Thank you

http://www.math.mcmaster.ca/∽mmehra